Sphingolipid synthesis is necessary for kinetoplast segregation and cytokinesis in *Trypanosoma brucei*

Alina Fridberg[1], Cheryl L. Olson[1], Ernesto S. Nakayasu[2], Kevin M. Tyler[3], Igor C. Almeida[2] and David M. Engman[1,*]

[1]Departments of Pathology and Microbiology-Immunology, Feinberg School of Medicine, Northwestern University, Chicago, IL 60611, USA
[2]Department of Biological Sciences, University of Texas at El Paso, El Paso, TX 79968, USA
[3]BioMedical Research Centre, School of Medicine, Health Policy and Practice, University of East Anglia Norwich, Norfolk, NR4 7TJ, UK
*Author for correspondence (e-mail: d-engman@northwestern.edu)

Accepted 13 November 2007
Journal of Cell Science 121, 522-535 Published by The Company of Biologists 2008
doi:10.1242/jcs.016741

Summary

Sphingolipids and their metabolites have been thought crucial for cell growth and cell cycle progression, membrane and protein trafficking, signal transduction, and formation of lipid rafts; however, recent studies in trypanosomes point to the dispensability of sphingolipids in some of these processes. In this study, we explore the requirements for de novo sphingolipid biosynthesis in the insect life cycle stage of the African trypanosome *Trypanosoma brucei* by inhibiting the enzyme serine palmitoyltransferase (SPT2) by using RNA interference or treatment with a potent SPT2 inhibitor myriocin. Mass spectrometry revealed that upon SPT2 inhibition, the parasites contained substantially reduced levels of inositolphosphorylceramide. Although phosphatidylcholine and cholesterol levels were increased to compensate for this loss, the cells were ultimately not viable. The most striking result of sphingolipid reduction in procyclic *T. brucei* was aberrant cytokinesis, characterized by incomplete cleavage-furrow formation, delayed kinetoplast segregation and emergence of cells with abnormal DNA content. Organelle replication continued despite sphingolipid depletion, indicating that sphingolipids act as second messengers regulating cellular proliferation and completion of cytokinesis. Distention of the mitochondrial membrane, formation of multilamellar structures within the mitochondrion and near the nucleus, accumulation of lipid bodies and, less commonly, disruption of the Golgi complex were observed after prolonged sphingolipid depletion. These findings suggest that some aspects of vesicular trafficking may be compromised. However, flagellar membrane targeting and the association of the flagellar membrane protein calflagin with detergent-resistant membranes were not affected, indicating that the vesicular trafficking defects were mild. Our studies indicate that sphingolipid biosynthesis is vital for cell cycle progression and cell survival, but not essential for the normal trafficking of flagellar membrane-associated proteins or lipid raft formation in procyclic *T. brucei*.

Supplementary material available online at
http://jcs.biologists.org/cgi/content/full/121/4/522/DC1

Key words: *Trypanosoma*, Serine palmitoyltransferase, Lipid, Sterol, Lipid rafts, Cell cycle

Introduction

Trypanosoma brucei is the protozoan parasite that causes sleeping sickness in vast regions of sub-Saharan Africa. Metacyclic forms of *T. brucei* in the tsetse fly salivary gland are transmitted to the mammalian bloodstream when the insect takes a blood meal, and differentiate into bloodstream forms that replicate and persist in the mammalian host through the process of antigenic variation. Bloodstream forms taken up by a tsetse during a blood meal differentiate to procyclic forms in the fly midgut, and replicate before migrating to the salivary gland and becoming metacyclics, completing the life cycle (Vickerman, 1985). African sleeping sickness is a major public health problem, causing significant morbidity and mortality and preventing sustained economic growth in Africa (Pepin, 2007).

In eukaryotic cells, sphingolipids play important roles in normal cell membrane architecture, and protein trafficking and sorting (Funato et al., 2002; Gruenberg, 2001; Ikonen, 2001). Various sphingoid bases and their metabolites also act as second messengers in the heat-stress response, regulation of cell growth and cell cycle progression, and apoptosis (Dickson and Lester, 1999; Obeid et al., 2002). In addition, sphingolipids – together with hydroxysterols – are canonical components of lipid rafts, heterogeneous membrane microdomains also known as detergent resistant membranes (DRMs) that often serve as scaffolds to organize signal transduction mechanisms within the cell (Brown and London, 1998; Ikonen, 2001; Pike, 2003; van Meer and Lisman, 2002).

The sphingolipid biosynthesis pathway begins with a condensation of palmitoyl CoA with serine to form 3-ketodihydrosphingosine (3-KDS), a reaction catalyzed by the pyridoxal 5′-phosphate-dependent serine palmitoyltransferase (SPT), a heterodimeric enzyme composed of two subunits, SPT1 and SPT2, both of which are essential for enzyme function (Hanada, 2003). Mutations in the SPT2 subunit in *Saccharomyces cerevisiae* and in Chinese hamster ovary cells that render the cells deficient in synthesis of sphingoid bases lead to severe growth retardation and eventual cell death unless the cells are supplemented with exogenous sphingoid bases (Dickson and Lester, 1999; Hanada, 2003; Pinto et al., 1992). Deletion of SPT2 in *Drosophila* leads to embryonic lethality (Dickson and Lester, 1999; Obeid et al., 2002).

The involvement of SPT in several aspects of cell activity has been well characterized in yeast, where sphingolipid synthesis in the endoplasmic reticulum (ER) is required for efficient transport

of glycosylphosphatidylinositol (GPI)-anchored proteins from the ER to the Golgi complex. Treatment with the SPT2 inhibitor myriocin, or mutation of the SPT1 subunit cause the GPI-linked protein Gas1p to accumulate in the ER. In yeast, ceramide-rich lipid rafts form in the ER, and disruption of these rafts is responsible for the reduced rate of transport of cholesterol and raft-associated proteins Gas1p, Pma1p and Nce2p from the ER to the cell surface (Bagnat et al., 2000; Bagnat and Simons, 2002; Funato et al., 2002; Perry, 2002). SPT1 temperature-sensitive mutants are deficient in receptor-mediated endocytosis (Zanolari et al., 2000), and downstream sphingoid bases, such as dihydrosphingosine (sphinganine), act as signaling molecules regulating endocytosis (Dickson and Lester, 1999). Finally, a temperature-sensitive SPT1 mutant deficient in sphingolipid synthesis lacks the transient heat-induced G0-G1 cell cycle arrest seen normally upon heat stress (Jenkins and Hannun, 2001).

Long-chain bases downstream of 3-ketodihydropshingosine also regulate cell cycle progression. Sphingosine can activate ERK to stimulate mitogenesis and proliferation in glomerular mesaglial cells, whereas ceramide stimulates JNK to suppress growth (Coroneos et al., 1996); in airway smooth muscle cells, by contrast, sphingosine elicits growth arrest via JNK and sphingosine phosphate stimulates DNA synthesis via ERK2 (Pyne et al., 1996). In microglial cells, acumulation of the sphingoid base psychosine uncouples mitotic and cytokinesis events, leading to formation of multinucleate cells (Kanazawa et al., 2000). In addition, ganglioside GM1 and cholesterol-enriched domains in the cleavage furrow of sea urchin eggs help create signaling platforms that containing activated Src and PLCγ, which are essential for cytokinesis (Ng et al., 2005).

Intriguingly, whereas sphingolipid biosynthesis and SPT activity are crucial in yeast and humans, in the kinetoplastid protozoan *Leishmania major* targeted deletion of the *SPT2* gene and the resulting block of sphingolipid biosynthesis are not lethal as long as the parasites are supplemented with ethanolamine (Denny et al., 2004; Denny and Smith, 2004; Zhang et al., 2005; Zhang et al., 2007; Zhang et al., 2003). Even in the absence of ethanolamine, only modest vesicular trafficking defects, cell shape abnormalities and reduced growth rate were observed in promastigotes, with the vast majority of the parasites dying only upon differentiation into metacyclic forms, probably owing to the extra demands on the vesicular trafficking pathway to accommodate the changes to cell physiology during transformation. Also notable is that surface lipid rafts still formed in *SPT2*-null *Leishmania* cells (Zhang et al., 2003; Denny et al., 2004), although the association kinetics of the GPI-linked protein GP63 with the ER rafts were delayed in one study (Denny et al., 2004). It is thought that three properties of the *Leishmania* membrane may allow lipid rafts to form even in the absence of sphingolipids: (1) ergosterol is the predominant β-hydroxysterol, which forms larger and more thermostable rafts than does cholesterol (Xu et al., 2001). (2) The glycoinositolphospholipids (GIPLs) may be upregulated to compensate for sphingolipid deficiency and, (3) GPI-linked raft-associated molecules are abundant in the plasma membrane. Intriguingly, sphingolipid biosynthesis is not essential for exocytosis in bloodstream forms of *T. brucei* or HeLa cells (Sutterwala et al., 2007).

The surface membrane of procyclic *T. brucei*, like those of *Leishmania* and fungi, contains inositolphosphorylceramide (IPC) in addition to sphingomyelin (Patnaik et al., 1993). Similar to other kinetoplastids, procyclic *T. brucei* can synthesize ergosterol but can also efficiently scavenge cholesterol if it is available (Coppens and Courtoy, 1995; Coppens and Courtoy, 2000), whereas the bloodstream forms primarily rely on cholesterol scavenging for survival. The flagellar membrane of *T. brucei* is highly enriched in lipid rafts, which permits the selective flagellar membrane targeting of a family of dually acylated proteins, the calflagins (our unpublished work). Like the coat of *Leishmania*, the membrane surface of *T. brucei* contains an abundance of GPI-linked proteins – procyclin in the insect form and variant surface glycoprotein (VSG) in the bloodstream form. However, neither procyclin nor VSG is associated with DRMs (Denny et al., 2001) (our unpublished work), probably owing to the unusual positions of the acyl chains on the inositol ring in the case of procyclin (Treumann et al., 1997) and the short acyl chain length of the anchor in VSG (Benting et al., 1999). Considering that the two related kinetoplastids both possess lipid rafts and synthesize ergosterol, but have GPI-anchored molecules with different biochemical properties, we wished to assess whether sphingolipid synthesis is similarly dispensable in *T. brucei*.

By inducing TbSPT2-specific RNA interference (RNAi) or inhibiting SPT2 with myriocin we found that, in contrast to what is observed in *Leishmania*, sphingolipid biosynthesis is required for the viability of *T. brucei*. It is essential for correct cell cycle progression because cells depleted of TbSPT2 and sphingolipids fail to undergo cytokinesis normally, yet continue through multiple rounds of DNA and organelle replication. Vesicular trafficking is only mildly affected, with defects emerging only after prolonged induction of TbSPT2 RNAi. Further, sphingolipid biosynthesis is not a requirement for lipid raft formation in procyclic parasites, although it is important in the bloodstream-stage of the organism. The differences in the requirements for sphingolipid biosynthesis between *T. brucei* and *Leishmania* may provide an interesting avenue to systematically analyse how differences in kinetoplastid life cycle and membrane composition contribute to parasite cell regulation.

Results

Identification of genes encoding the subunits of *T. brucei* serine palmitoyltransferase and construction of RNAi lines

The *T. brucei* genes *SPT1* (Tb927.4.1020, hereafter referred to as *TbSPT1*) and *SPT2* (Tb10.70.3220, hereafter referred to as *TbSPT2*) were identified in the *T. brucei* genome database (www.genedb.org). Both genes are present in two allelic copies. *TbSPT1* is found on chromosome 4 and is 1473 bp in length; *TbSPT2* is found on chromosome 10 and is 1674 bp in length. TbSPT1 and TbSTP2, respectively, display sequence identity (in percent) with SPT proteins of the following species: *Trypanosoma cruzi* SPT1 55% and SPT2 64%, *Leishmania major* SPT1 66% and SPT2 57%, *Saccharomyces cerevisiae* SPT1 25% and SPT2 34%, *Homo sapiens* SPT1 and SPT2 both 37% each (see supplementary material Fig. S1). The *Leishmania SPT1* and *SPT2* genes (referred to as *LmSPT1* and *LmSPT2*, respectively) are closely related phylogenetically to their *T. brucei* and *T. cruzi* counterparts (Denny et al., 2004; Zhang et al., 2003).

Northern blot analysis of RNA derived from *T. brucei* bloodstream and procyclic forms revealed that expression of *TbSPT2* is higher in the latter life cycle stage of the parasite (Fig. 1A). SPT1 and SPT2 function as a heterodimer and deletion of LmSPT2 abolishes the function of the protein (Denny et al., 2004; Zhang et al., 2003). TbSPT2 contains the catalytic site motif (G381-MGTFTKSFG-G389), within which K386 is thought to

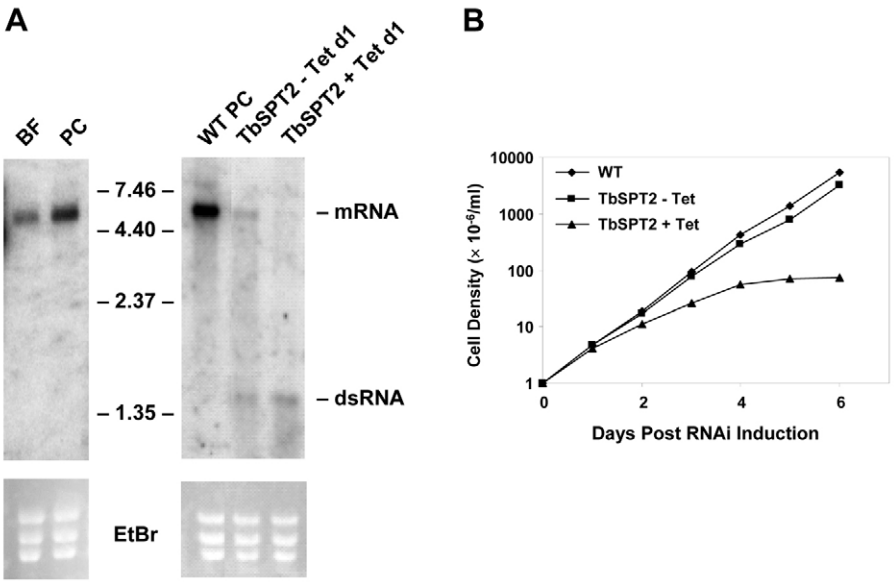

Fig. 1. Inhibition of TbSPT2 causes growth arrest in *T. brucei*. (A) *TbSPT2* expression in bloodstream (BF) and procyclic (PC) stage parasites was analyzed by northern blot hybridization. RNAi was induced in a procyclic cell line containing an integrated copy of the RNAi construct pZJM-TbSPT2 by the addition of 1 μg/ml Tet. *TbSPT2* RNA levels were compared at day 1 post induction (TbSPT2 +Tet d1) with those in cells of the 29-13 cell line and in uninduced transfectants (TbSPT2–Tet d1). Ethidium bromide (EtBr)-stained gels are shown beneath the northern blots and the positions of molecular size standards are indicated (in kb). (B) The in vitro growth of the TbSPT2 RNAi cell line was assessed in the presence or absence of Tet induction and compared with that of the 29-13 line. Cultures of the three parasite lines were initiated in SDM79 medium at a density of 10^6 cells/ml and culture densities were determined daily for 6 days.

bind the essential cofactor pyridoxal 5′-phosphate (Hanada, 2003). For these reasons, we decided to target *TbSPT2* to disrupt SPT function and sphingolipid synthesis in *T. brucei*. To determine the effects of sphingolipid depletion on the physiology of *T. brucei*, we generated a TbSPT2 RNAi cell line in the procyclic form of the parasite. To do so, we cloned 735 bp of the *TbSPT2* gene into the *T. brucei* RNAi vector pZJM (Wang et al., 2000), which produces double-stranded (ds)RNA when induced with tetracycline (Tet), and inserted the vector into a modified procyclic cell line (29-13) containing a Tet promoter and a T7 polymerase repressor to regulate transcription. Induction of *TbSPT2* RNAi in procyclic cells resulted in a significant decrease in the level of the *TbSPT2* mRNA 1 day after induction (Fig. 1A). Although the construct expresses dsRNA at a low but significant level in the absence of Tet, as previously reported (Alibu et al., 2005) the uninduced procyclic TbSPT2 RNAi cell line had only a slightly longer doubling time compared with the parental 29-13 cell line in the absence of Tet (Fig. 1B). Upon induction of *TbSPT2* RNAi, the cells stopped dividing over a period of 5-6 days, lost motility and began to die, as indicated by 4′,6′-diamidino-2-phenylindole hydrochloride (DAPI)-exclusion staining (Van der Linden and Deelder, 1984) (data not shown). A 16-hour treatment of the parental 29-13 procyclic cells and the 90-13 bloodstream cells with myriocin – a fungal inhibitor that targets SPT2 (Miyake et al., 1995) – at concentrations of 0.5-5 μM and 0.05-0.5 μM, respectively, also resulted in cell death as assessed by DAPI permeability of living cells. Several attempts to generate a bloodstream TbSPT2 RNAi line were unsuccessful.

Reduction of de novo sphingolipid synthesis and sphingolipid levels, and an increase in cholesterol uptake is seen in *TbSPT2* RNAi +Tet and myriocin-treated parasites

To confirm that TbSPT2 targeting blocks de novo sphingolipid synthesis, we employed both an RNAi approach and myriocin treatment. TbSPT2 RNAi cells were left uninduced (TbSPT2 –Tet) or induced with tetracycline (TbSPT2 +Tet) for 3 days. 29-13 cells were either left untreated (WT) or treated for 1 day with 1.5 μM myriocin (WT +Myr), which reduced cell division and produced physiological abnormalities closely resembling those observed in TbSPT2 RNAi +Tet cells (data not shown and Fig. 3B,C). All cells were then pulse-labeled with [3H] serine and lipids were extracted and analyzed by thin-layer chromatography (TLC) (Fig 2). Ceramide was distinguished from phosphatidylserine (PS) and phosphatidylethanolamine (PE) by mobility from the origin and comparison with ceramide, PS and PE standards. Labeled ceramide was found in abundance in the control 29-13 and uninduced TbSPT2 RNAi lines but was not found in 29-13 cells treated with myriocin, and ceramide labeling was substantially reduced in TbSPT2 RNAi cell lines induced with Tet. Thus, inhibition of TbSPT2 by either method resulted in reduced levels of sphingolipid synthesis.

To determine which specific lipids are reduced upon SPT inhibition, we analyzed total lipid fractions, obtained by Folch's partition, employing electrospray-ionization quadrupole time-of-flight (ESI-QTOF) tandem mass spectrometry (MS/MS) in the negative-ion mode (Fig. 3). Individual parent ions were subjected to collision-induced dissociation, and the resultant MS/MS spectra were analyzed to identify the lipid species (supplementary material Fig. S2). Analysis of the MS/MS spectra clearly showed that most ion species between the mass to charge ratio (*m/z*) 750 and 870 are *myo*-inositol (*m*I)-containing phospholipids, because an abundant and characteristic daughter ion at *m/z* 241.0, which corresponds to *myo*-inositol-cyclic phosphate (mI_cP), was observed in most fragmented ions (see supplementary material Fig. S2). The ion species at *m/z* 750.5, 778.5, and 806.6 showed a poor fragmentation profile, typical of inositolphosphorylceramides (IPCs) in negative ion-mode ESI-MS/MS, where only daughter ions corresponding to mI_cP and *myo*-inositol-phosphate (*m*IP) were observed (supplementary material Fig. S2A). The IPC species at *m/z* 750.5 and 752.5 most probably correspond to C14:0/d18:1-IPC and C14:0/d18:0-IPC, respectively, and the species at *m/z* 778.5 and 780.5 to C16:0/d18:1-IPC and C16:0/d18:0-IPC, respectively. Furthermore, the minor ion species detected at *m/z* 806.6 or 806.5 in the top three spectra (29-13, 29-13+Myr, and TbSPT2–Tet) of Fig. 3, most probably correspond to C18:0/d18:1-IPC (Figs 3, supplementary material Fig. S2A, bottom spectrum). Nevertheless, because we could not assign the specific sphingoid bases and fatty

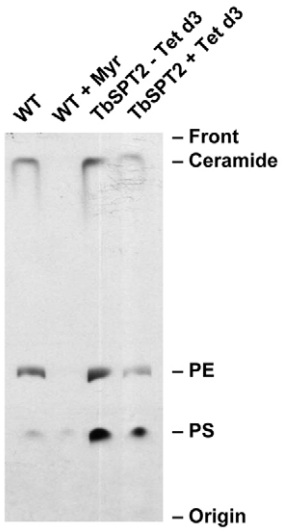

Fig. 2. Sphingolipid biosynthesis is reduced by myriocin treatment or TbSPT2 RNAi. The *T. brucei* 29-13 cell line was grown in the absence or presence of myriocin (1.5 μM) for 1 day; TbSPT2 RNAi cells were grown for 3 days in the presence or absence of Tet and pulse-labeled with [^{3}H]serine for 40 minutes. Lipids were extracted using the Blight-Dyer method and resolved by TLC and visualized by autoradiography. Each lane contains material from 5×10^8 cells. Positions of phosphatidylethanolamine (PE) and phosphatidylserine (PS) and ceramide standards are indicated.

acids in any of the IPC species, further biochemical characterization of the ceramide moiety of these ion species remains to be carried out. It is noteworthy that IPC species at *m/z* 750, 752, 778 and 780 were also recently identified in *T. brucei*, and assigned as C32:1-IPC, C32:0-IPC, C34:1-IPC and C34:0-IPC, respectively (Guther et al., 2006). Moreover, the IPC species corresponding to C16:0/d18:1-IPC and C16:0/d18:0-IPC were also found to be major free IPC species in *T. cruzi* (Bertello et al., 1995) (I.C.A., unpublished results).

By contrast, the ion species at *m/z* 835.6, 861.6 and 863.6 (Fig. 3) gave rise to a rich fragmentation profile typical of phosphatidylinositols (PIs), where daughter ions corresponding to carboxylate ions of fatty acids (at *m/z* 255.3, 279.3 and 281.3) and glycerol-cyclic phosphate (Gro_cP) were observed among several other ions (supplementary material Fig. S2B). The major PI species at *m/z* 861.4 and 863.5 were then assigned as C18:0/C18:2-PI and C18:0/C18:1-PI, respectively, both of which were also abundantly found in all *T. cruzi* life cycle stages (I.C.A., unpublished data).

After the identification of the phospholipid species, we monitored the decrease of IPC levels in myriocin-treated or TbSPT2 RNAi +Tet parasites by comparing the relative abundance of the IPC ions to those corresponding to major PI species at *m/z* 835.6, 861.6, and 863.6. A clear reduction in the levels of all five species of IPC (at *m/z* 750.5, 752.5, 778.5, 780.5 and 806.5) was observed after treatment with myriocin (Fig. 3; 29-13 + Myr). Compared with the myriocin treatment, the TbSPT2 RNAi induction (TbSPT2 + Tet) also markedly affected the synthesis of all IPC species (at *m/z* 750.5, 752.5, 778.5 and 780.5). In addition, because the relative abundance of the major PI species (at *m/z* 835.6, 861.6 and 863.6) appeared not to be altered by the two treatments, particularly with myriocin, this may indicate that sphingolipid biosynthesis was selectively inhibited in both cases. On the one hand, we found that the ion species at *m/z* 806.5, 808.5, 816.5, 818.5, 820.5 and 822.5, which are substantially increased upon SPT2 RNAi induction (Fig. 3; SPT2 + Tet), are in fact phosphatidylcholine (PC) species with a Cl^- adduct (supplementary material Fig. S2C). On the other hand, the ion species at *m/z* 847.5, which was also augmented upon SPT2 RNAi induction, was assigned as 1-*O*-C18:0-alkyl-2-*O*-18:2-acyl-PI (supplementary material Fig. S2C). This ion species has also been described previously (Guther et al., 2006).

Since sterols are also an integral part of membrane architecture (Coppens and Courtoy, 1995; Coppens and Courtoy, 2000), and because *T. brucei* can both synthesize ergosterol and efficiently scavenge cholesterol from the cell culture medium (Coppens and Courtoy, 1995; Coppens and Courtoy, 2000; Zhou et al., 2007), we examined whether cells with reduced TbSPT2 activity increase their sterol levels to compensate for sphingolipid depletion. To this end, we employed gas chromatography (GC)-MS analysis, using the plant sterol sitosterol as an internal standard, and cholesterol, lanosterol and ergosterol as external standards, to determine the type and amount of sterols present in these cells (Table 1 and supplementary material Fig. S3). The major *T. brucei* sterols detected in the 29-13 sterol fraction were cholesterol (Cho), cholesteryl esters (ChoE), and lanosterol (Lan), a precursor of ergosterol (Table 1 and supplementary material Fig. S3). In 29-13 cells treated with 1.5 μM myriocin, the absolute amount of Cho and ChoE per cell increased two- to threefold, and the Cho:Lan ratio increased twofold as well, indicating that – rather than significantly relying on the ergosterol synthesis pathway – myriocin-treated cells attempt to compensate for decreased sphingolipid levels by taking up more Cho and ChoE from the cell culture medium. Also intriguingly, in comparison with 29-13 cells, TbSPT2 RNAi –Tet cells show an almost 4.5-fold increase in total cell cholesterol, which is paralleled by a fivefold increase in the Cho:Lan ratio. This

Table 1. Myriocin-treated 29-13 cells and the TbSPT2 RNAi line contain elevated cholesterol levels relative to the control 29-13 cell line

	Cholesterol (Cho)		Cholesteryl ester (ChoE)		Lanosterol (Lan)		
T. brucei cell line	picomoles per 10^7 cells	% of total	picomoles per 10^7 cells	% of total	picomoles per 10^7 cells	% of total	Ratio of Cho:ChoE:Lan
29-13 WT	19.7±0.9	59.7	7.3±0.1	22.1	6.0±0.3	18.2	3.3:1.2:1.0
29-13 + Myr	55.7±7.3	68.9	15.6±0.2	19.3	9.5±0.4	11.7	5.9:1.6:1.0
TbSPT2 – Tet	98.0±1.7	88.1	7.1±0.2	6.4	6.2±1.5	5.6	15.8:1.1:1.0
TbSPT2 + Tet	46.3±3.0	77.8	7.0±0.3	11.8	6.2±0.0	10.4	7.4:1.1:1.0

Sterols extracted by the modified Folch's method and purified using the column with silica-gel resin were analyzed by GC-MS using Sit as an internal standard, and Cho, Lan and Erg as external standards to determine the type and amount of sterols present in the cells. The major *T. brucei* sterols detected were Cho, ChoE and Lan, a precursor of ergosterol. The absolute concentration of each sterol in the cell, percent of each sterol to total sterol content and the ratios of Cho:ChoE:Lan are indicated. ChoE was considered as having the same molar response as Cho.

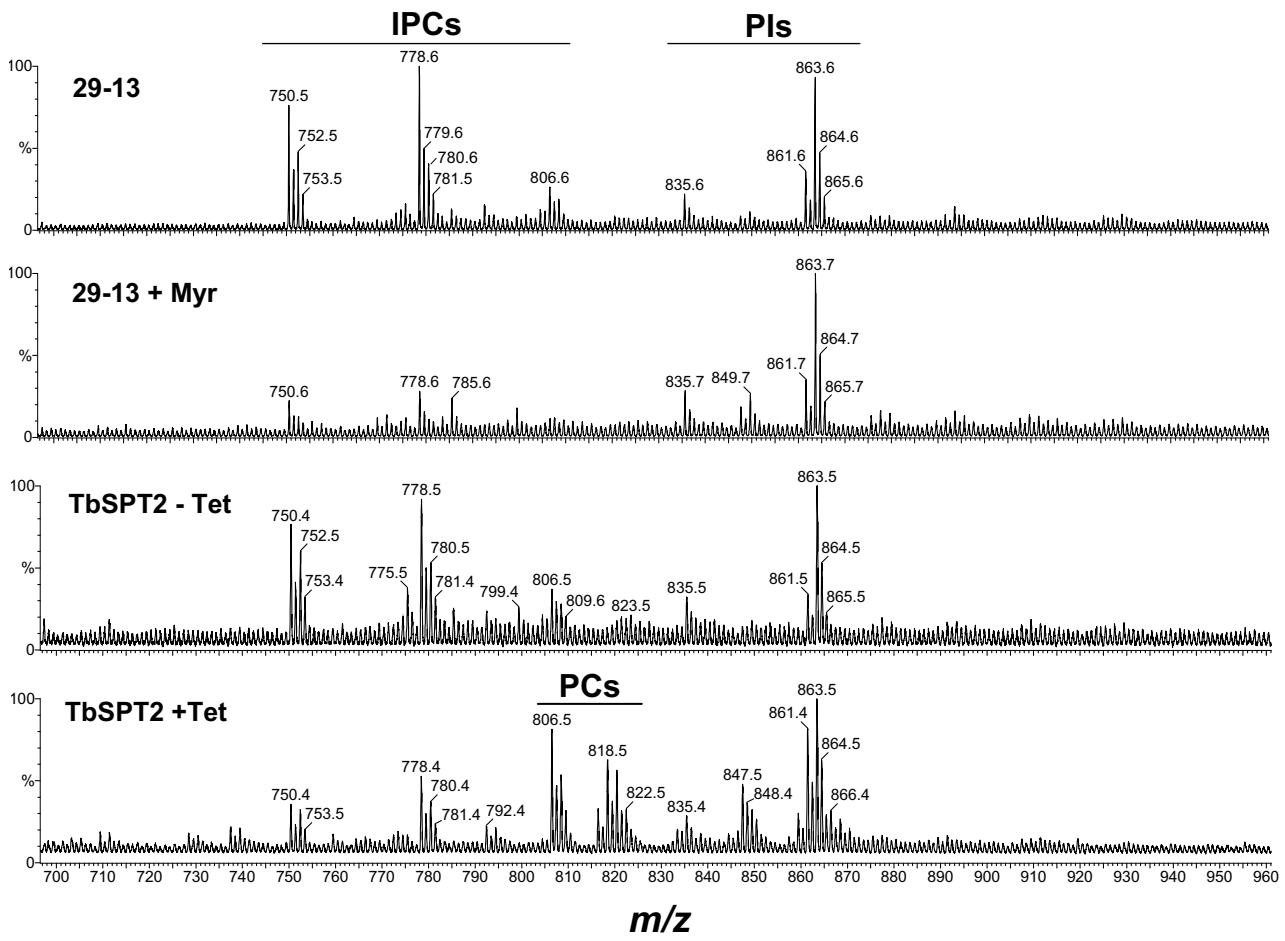

Fig. 3. Sphingolipid levels are reduced in the TbSPT2 RNAi cell line and in the 29-13 *T. brucei* cell line treated with myriocin (Myr). Negative-ion mode ESI-MS spectra of total lipids obtained from procyclic *T. brucei* are shown. 29-13, procyclic 29-13 cell line; 29-13 + Myr, 29-13 cell line treated with 1.5 μM myriocin; TbSPT2 + Tet, SPT2-RNAi-induced transfectant cells; TbSPT2–Tet, SPT2-RNAi-uninduced transfectant cells. *m/z*, mass to charge ratio; IPCs, inositolphosphorylceramides; PIs, phosphatidylinositols.

suggests that, because the RNAi construct is 'leaky' and some mRNA is being degraded even in uninduced cells (Fig. 1), the TbSPT2 RNAi –Tet cell line may have adopted a long-term strategy to compensate for reduction in sphingolipid levels by extra cholesterol scavenging. By comparison, the TbSPT2 RNAi +Tet cells, while showing more than a twofold increase in total cell Cho and Cho:Lan ratios over 29-13 cells, have a twofold lower ratio of Cho:Lan as compared to TbSPT2 –Tet cells. This suggests that since, at day 3 post induction, TbSPT2 RNAi +Tet cells are less healthy than their –Tet counterparts, their cholesterol uptake rate may be slowed, and/or that the upregulation in PC synthesis (Fig. 2) may further compensates for the bulk loss of sphingolipids. There is no increase in the ratio of ChoE:Lan between TbSPT2 RNAi +Tet and –Tet cells in comparison with the parental 29-13 cells. Surprisingly, we were able to detect lanosterol but not significant quantities of ergosterol in the 29-13 fraction, possibly owing to differences in extraction methods between our study and that of the Nes group (Zhou et al., 2007).

Sphingolipid depletion leads to incomplete cytokinesis and delayed kinetoplast segregation

To understand the basis for growth arrest of the TbSPT2 RNAi line, we examined the cells by scanning electron microscopy (SEM), light microscopy and DNA content analysis (Fig. 4). TbSPT2 RNAi cells induced with Tet displayed a variety of aberrant cell phenotypes (Fig. 4A,C). At day 3 post induction, defective cytokinesis was observed, with many parasites displaying a 'stable' cleavage furrow or remaining fused after coming close to separation (Fig. 4A, day 3b and 3c and day 6). Furthermore, in a typical growing trypanosome cell, the new flagellum is attached along its length to the cell body via a cytoskeletal junction structure known as the flagellar attachment zone (Robinson et al., 1995), and also to the old flagellum at the anterior end via the flagella connector (Briggs et al., 2004; Moreira-Leite et al., 2001). Together, the structures of these complexes help guide cell morphogenesis and maintain the correct polarity of underlying cell structures as it prepares for cytokinesis (Briggs et al., 2004; Moreira-Leite et al., 2001; Ngo et al., 1998; Robinson et al., 1995) and help define the site of cleavage furrow initiation (Kohl et al., 2003). In some TbSPT2 RNAi +Tet cells, the growing daughter flagellum was not connected to the old flagellum either at the tip or across partial or full length of the cell body (Fig. 4A, day 3c), which may have been partially responsible for some of the incorrect initiation or completion of cytokinesis found at this and later time points. Also, in contrast to a normally dividing procyclic cell, in which the daughter flagella emerge from a separate flagellar

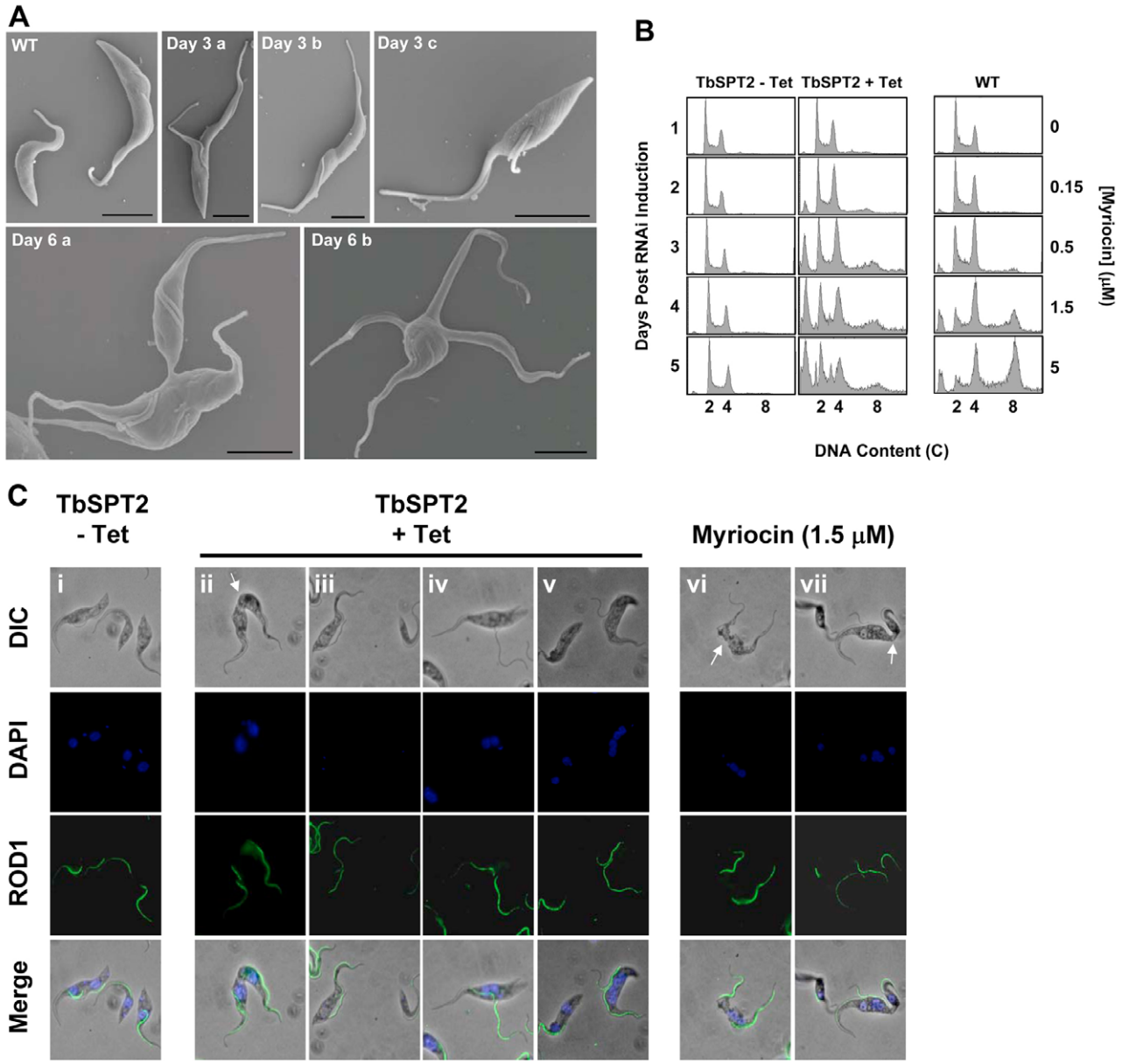

Fig. 4. Polymorphic phenotype of the TbSPT2 RNAi line. (A) Scanning electron micrographs of TbSPT2 RNAi cells grown for either 3 or 6 days in the presence of Tet. Compared with 29-13 (WT) cells, many TbSPT2 RNAi +Tet cells showed incomplete cytokinesis (Days 3a and 3b). In some TbSPT2 RNAi +Tet cells, the parental and daughter flagella both emerged from the same flagellar pocket, with the daughter flagellum partially detached from the parent flagellum and the cell body (Day 3c). At day 6 post Tet induction, many enlarged TbSPT2 RNAi cells containing polyflagellated extensions were observed (Days 6a and b). (B) DNA content analysis of the TbSPT2 RNAi line with (+) or without (–) Tet over 5 days of treatment. The *x*-axis shows the DNA content, measured by intensity of fluorescence emission at 440 nm. The *y*-axis shows the number of cells. The number of cells with a DNA content of 4C increased on days 1-2; number of cells with a DNA content of >4C and <2C increased progressively on days 3-5. The same was observed upon treating the cells with increasing concentrations of myriocin for 24 hours. (C) TbSPT2 RNAi –Tet and +Tet cells at day 3, and 29-13 cells treated with 1.5 μM myriocin for 24 hours were analyzed by immunofluorescence microscopy by using antiserum specific for the paraflagellar rod (ROD1). Cells were also visualized by phase microscopy and by using DAPI staining. (i) control TbSPT2 RNAi–Tet. (ii-v) TbSPT2 RNAi + Tet. (vi-vii) 29-13 cells treated with 1.5 μM myriocin. Both treatment conditions produced similar phenotypes, with TbSPT2 RNAi +Tet cell images being representative of myriocin-treated cells and vice versa. (ii) A cell stuck partway through cytokinesis, undergoing another round of DNA replication. Note that the kinetoplast has already been re-segregated in the upper part of the cell. (iii) Double (0N2K) zoids (left) and single (0N1K) zoids (right) – anucleate cells with two or one kinetoplasts, respectively; the 0N2K-zoid has a partially detached daughter flagellum. (iv) 2N1K* cell (containing an undivided kinetoplast) with a detached daughter flagellum. (v) A 2N1K cell (left) and a 4K2N cell with a detached flagellum (right). (vi) A 2N2K cell with a mispositioned cleavage furrow that can give rise to a zoid and a 2N1K cell. (vii) A 4N3K cell with one undivided kinetoplast, one detached flagellum, and a cytoplasmic tether. Arrows indicate cleavage furrows and cytoplasmic tethers.

pocket early after flagellar nucleation, the flagellar pocket failed to divide in a small portion of the SPT2 RNAi +Tet cells. By day 6, most cells appeared to have undergone multiple rounds of growth despite being defective in cytokinesis, resulting either in giant cells with multiple cleavage furrows and cytoplasmic tethers (Fig. 4A, day 6a) or in a central spherical cell mass from which multiple independent cytoplasmic extensions bearing flagella radiate (Fig. 4A, day 6b). Overall, these data suggest that sphingolipids are

necessary for completion of cytokinesis and may also act as signals for cellular proliferation.

Analysis of cellular DNA content by flow cytometry indicated that, at days 1 and 2 post TbSPT2 RNAi induction, the number of parasites in G1-S stage of the cell cycle (2C DNA content) is reduced and the parasites progressively accumulate in G2-M phase of the cell cycle (4C DNA content), whereas cells with elevated (>4C) or reduced (<2C) DNA content become more common by day 3 (Fig. 4B). By day 5, the DNA content varied widely, from <2C to >8C, reflecting the highly heterogeneous appearance of the cells observed by SEM. Treatment of the procyclic 29-13 cell lines with a range of myriocin concentrations for 24 hours resulted in a similar phenotype (Fig. 4B), and increasing the amount of myriocin from 0.5 μM to 5 μM also increased the DNA content of cells from <2C to >4C, paralleling the phenotype seen during TbSPT2 RNAi induction. One marked difference was that the peak DNA content of 8C was more pronounced in myriocin-treated cells than in TbSPT2 RNAi lines, where DNA content of >4C was more varied. A more gradual sphingolipid synthesis inhibition in RNAi experiments versus myriocin treatment probably allowed the TbSPT2 RNAi parasites a greater time span in which to initiate and partially complete multiple rounds of cytokinesis.

We used DAPI staining and immunofluorescence microscopy to observe and quantify the nuclear and kinetoplast structure of aberrant cells in the TbSPT2 RNAi line (Fig. 4C and supplementary material Fig. S4). As expected from flow cytometry analysis, the number of cells with one nucleus and one kinetoplast (1N1K), corresponding to the G1 stage of the cell cycle, decreased substantially between days 0 and 3 post induction, from 73% to 39%, and the number of cells with one nucleus and two kinetoplasts (1N2K), corresponding to S phase, decreased from 13% to 6% (supplementary material Fig. S4). 2N2K cell numbers rose from 10% to 15% at day 3, approximately half of those clearly initiated cytokinesis and showed a 'paused' or incomplete ingression of the cleavage furrow (Fig. 4A, day 3a-b).

A big increase was seen in three populations. Numbers of 0N1K parasites, known as 'zoids' – anucleate cells with a single kinetoplast, typically produced from a mispositioned cleavage furrow during cytokinesis of 2N2K cells (Ploubidou et al., 1999) – rose from 1% to 12%, and accounted in part for the peak of <2C DNA content observed by flow cytometry (Fig. 4Ciii). However, we also observed zoids arising from cells with >4C DNA content (data not shown), as well as the presence of 'double zoids' (0N2K, anucleate cells with two kinetoplasts; less than 1% of the cell population), arising from cells in which kinetoplasts were in close proximity or in the process of dividing during cytokinesis (Fig. 4viii).

The number of 2N1K cells increased from 1% to 14%. In addition to cells that represented 'zoid partners' – the complement of 0N1K-zoids arising from 2N2K cells (Ploubidou et al., 1999) (Fig. 4Cv), ~30% of the 2N1K population at day 3 contained a single elongated or enlarged kinetoplast (2N1K*) (Fig. 4Ciii), although this particular defect was not as apparent at days 1 and 2 (data not shown). Staining the cells with ROD1, an antibody specific for the paraflagellar rod, a flagellum-specific cytoskeletal structure, showed that the 2N1K* cells contained two flagella 75% of the time. Daughter flagella were either fully or partially detached from the cell body in 70% of this subset of the population, and two flagella were associated with the same kinetoplast 5% of the time (data not shown). The presence of the new flagellum but only a single enlarged kinetoplast suggest that the basal bodies associating with the flagellum were able to replicate but not segregate, causing the fused or divided but mispositioned kinetoplasts. A similar phenotype in *T. brucei* has recently been reported for cells overexpressing the Polo-like kinase TbPLK (Hammarton et al., 2007). This also correlated with the presence of cells with two flagella emerging from a single flagellar pocket observed by SEM. Further, 30% of the 2N2K cells also contained a detached daughter flagellum but no clear cleavage furrow ingression, suggesting that they arose from 2K1N* cells. Presumably, this cell population did not initiate cytokinesis because mitochondrial DNA segregation and flagellar attachment are required for these events (Kohl et al., 2003; LaCount et al., 2002; Robinson and Gull, 1991).

The number of XNXK cells (DNA content >4C, where X is >2C) increased from 1% to 14%. Asynchronous DNA replication and segregation could be observed across the cleavage furrow (Fig. 4Cii), very similar to a phenotype previously reported in *T. brucei* for RNAi of the receptor for activated C kinase 1 (Rothberg et al., 2006). Because of aberrant cytokinesis, asynchronous DNA replication, and delay in kinetoplast division, XNXK cells did not always contain equal numbers of nuclei and kinetoplasts (Fig. 4Cii,v) and, in some, enlarged undivided kinetoplasts and detached flagella were also seen. Polymorphic cells accounted for a large percentage of the population at day 6 (see supplementary material Movie 1). The same range of aberrant phenotypes was seen when treating cells of the procyclic 29-13 cell line with myriocin (Fig. 4Cvi and vii, and data not shown). Taken together, the data suggest that TbSPT2 is essential for completion of cleavage furrow formation and also impacts correct kinetoplast segregation in procyclic *T. brucei*.

Ultrastructural abnormalities of the TbSPT2 RNAi cell line

To examine the internal morphology in the TbSPT2 RNAi parasites, we compared the wildtype cells with the TbSPT2 RNAi line by thin-section transmission electron microscopy at three and six days post Tet induction. Consistent with our previous observations, in comparison with 29-13 cells (Fig. 5A), we observed multiple nuclei (Fig. 5C) and enlarged and sometimes misshapen kinetoplasts (Fig. 5B). At 3 days post Tet induction, lipid bodies in the cytoplasm of TbSPT2 cells (Fig. 5D,F,H) were observed 15 times more frequently in cross-sections of comparable area than in cells from the 29-13 line. Coiled multilamellar structures were frequently seen, appearing either contiguous with or within the mitochondrial membrane (Fig. 5E), or in close proximity to the nucleus (Fig. 5G). The Golgi complex appeared fragmented in some of the cells (Fig. 5F) although this was not seen in all cells (Fig. 5G). However, the acidocalcisomes appeared normal, and there was no accumulation of vesicles within the cytosol of the parasite, as has been previously observed in kinetoplastid cells with vesicular trafficking defects (Allen et al., 2003; Denny et al., 2004; Garcia-Salcedo et al., 2004; Zhang et al., 2003), indicating that, while some vesicular trafficking defects were present, they were mild. A distended mitochondrial membrane (Fig. 5D,F) was frequently observed, and coiled mitochondrial extensions were sometimes seen to surround the lipid bodies (Fig. 5D) or acidocalcisomes (data not shown). Some cells also contained a distended flagellar pocket (Fig. 5H and Movie 1). These phenotypes emerged by day 3 post induction, becoming more pronounced and frequent at day 6, when the numbers of cells with >4C DNA content were greatest. Overall,

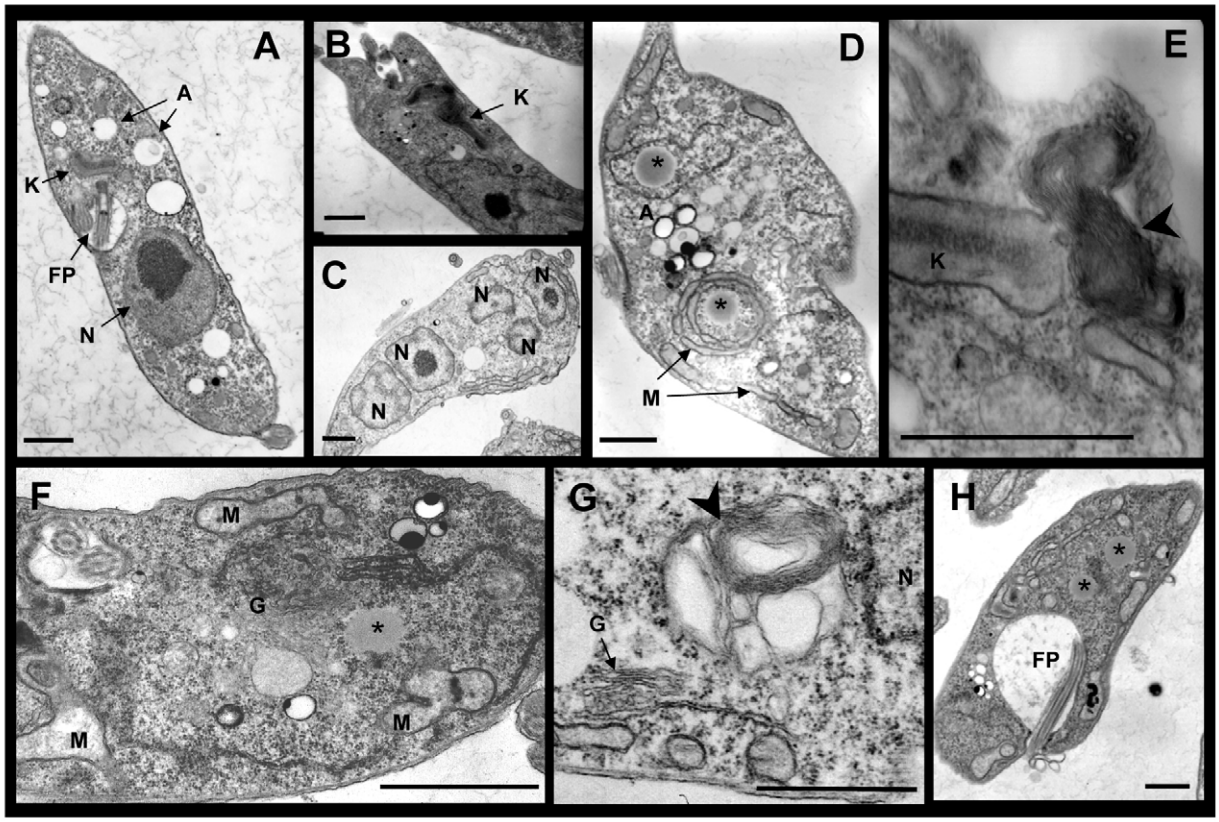

Fig. 5. Ultrastructural abnormalities of the TbSPT2 RNAi cell line. (A-H) Transmission electron microscopy images of (A) *T. brucei* 29-13 cells and of (B-H) cells of the TbSPT2 RNAi cell line grown for either 3 days (B,C) or 6 days (D-H) in the presence of Tet. Scale bars, 1 μm. (A) *T. brucei* 29-13 cell showing an undivided kinetoplast (K) next to the flagellar pocket (FP), a normal nucleus (N) and acidocalcisomes (A). (B) Cell with an abnormally large misshapen kinetoplast. (C) Cell with multiple nuclei. (D) Two cytoplasmic lipid deposits (*), one surrounded by the endoplasmic reticulum and one surrounded by a coiled mitochondrion (M). Mitochondrial distention is observed at the top and bottom aspects of the cell. Acidocalcisomes (center left) appear normal. (E) Multilamellar structure (arrowhead) contiguous with the kinetoplast (K) membrane. (F) Fragmented Golgi complex next to the ER, and several cross-sections of a distended mitochondrion. (G) Coiled multilamellar structure (arrowhead) next to the nucleus above the Golgi. The Golgi cross-section appears normal. (H) Distended flagellar pocket.

these phenotypes likely represent secondary defects stemming from the unusual demands placed on the cell by continued growth.

SPT2 RNAi growth and cytokinesis defects can be rescued with 3-KDS but not ceramide

Since SPT2 is responsible for the synthesis of 3-KDS, we wanted to determine whether sphingoid bases can rescue the TbSPT2 RNAi phenotype. We grew the cells with daily addition of 2.5-0.5 μM 3-KDS, as well as 1-20 μM of ceramide – a sphingoid base needed downstream in the synthesis pathway. 3-KDS was able to partially rescue the growth of the TbSPT2 RNAi line – increasing the growth of Tet-induced cells nearly tenfold (Fig. 6A) – and partially reverse the cell cycle progression defect (Fig. 6B and data not shown). However, it was not possible to reverse the phenotype completely. Addition of ceramides containing C18 fatty acids or fatty acids of mixed length at concentrations of 1-20 μM (Fig. 6A,B and data not shown) did not rescue the mutant phenotype. Observations in mammalian SPT-deficient mutant cell lines in yeast and *L. major* SPT2-null cells indicate that uptake and delivery of exogenous ceramide is inefficient (Denny et al., 2004; Hanada et al., 1992; Zhang et al., 2003), and this inefficient uptake may be also be responsible for lack of rescue in *T. brucei*. Higher concentrations of both 3-KDS and ceramide inhibited the growth of procyclic *T. brucei* (data not shown). Complementation with high concentrations of exogenous sphingoid bases has been observed to cause toxicity to mammalian cells and *S. cerevisiae* (Hanada, 2003; Obeid et al., 2002; Pinto et al., 1992).

Sphingolipid depletion does not affect flagellar lipid raft formation in procyclic forms

In most eukaryotic organisms, sphingolipids, together with hydroxysterols such as cholesterol or ergosterol, are crucial components of DRMs (Brown and London, 1998; Ikonen, 2001; Simons and Toomre, 2000; van Meer and Lisman, 2002). DRMs are present in both *Leishmania* (Denny et al., 2001) and *T. brucei*, and are enriched in the flagellum in *T. brucei* procyclic forms (K.M.T. et al., unpublished). The dually acylated Ca^{2+}-binding protein calflagin Tb24 associates with flagellar lipid rafts in *T. brucei* procyclics (K.M.T. et al., unpublished). We assessed calflagin localization in TbSPT2 RNAi cells at day 3 post induction, in the 29-13 cell line after 1 day of treatment with 1.5 μM myriocin, and in the bloodstream 90-13 cell line treated with 0.15-1.5 μM myriocin (Fig. 7A). Although in procyclic cells the phenotypic changes were pronounced under both treatment conditions, calflagin still localized to the multiple flagella in a manner similar to that of controls. Calflagin also still localized to the flagellum in bloodstream forms of the parasite.

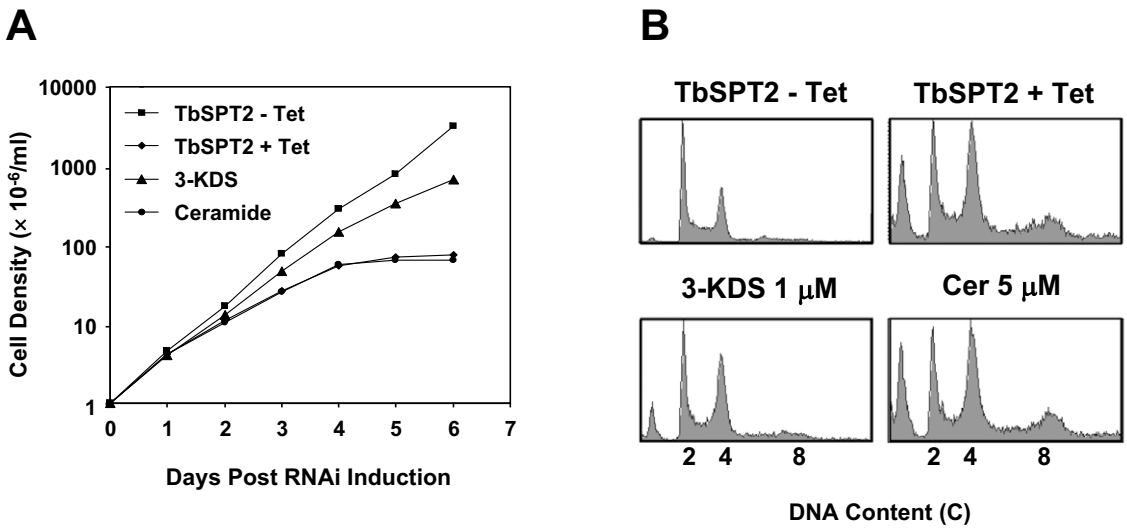

Fig. 6. TbSPT2 RNAi growth defect and cytokinesis defect can be rescued with 3-KDS, but not ceramide. (A) TbSPT2 RNAi cell lines grown in the presence of Tet were supplemented with either 1 μM 3-KDS or 5 μM C-18 ceramide (Cer) and compared with uninduced (–Tet) RNAi cells. Cultures were initiated in SDM79 medium at a density of 10^6 cells/ml and culture densities were determined daily for 6 days using a Coulter counter. TbSPT2 RNAi +Tet cells complemented with 3-KDS grow to ~ten times the number of those without 3-KDS. Ceramide complementation has no effect on cell number. (B) Flow cytometric analysis of DNA content of the TbSPT2 RNAi cell line complemented with 3-KDS and ceramide as described above, shown 3 days post Tet induction. To assess DNA content, timed samples were collected and stained with 20 μg/ml Hoechst dye solution containing 0.1% Triton X-100 and 0.5% formaldehyde, and analyzed using BD LSRII Flow Cytometer. Cell numbers are given at the *x*-axis, DNA content as measured by intensity of emission at 440 nm is given at the *y*-axis. A clear decrease in 2C DNA content and an increase in >4C and <2C DNA content is seen with addition of 3-KDS but not ceramide to TbSPT2 RNAi cell line induced with Tet.

One commonly used assay for determining whether a protein is associated with DRMs is sucrose-gradient fractionation of low-temperature-detergent lysates. We analyzed the association of calflagin with the DRM fraction in procyclic TbSPT2 RNAi cells cultured in the presence or absence of Tet for 3 days, as well as in cells of the procyclic 29-13 cell line cultured in the presence or absence of 1.5 μM myriocin for 1 day. In both cases, inhibition of sphingolipid synthesis did not affect the flotation of calflagin on the gradient within DRM fraction two or fraction three (Fig. 7B). However, in bloodstream form parasites treated with the lesser (0.15 μM) concentration of myriocin for 24 hours (which is enough to inhibit cell growth) calflagin no longer associated with DRMs (Fig. 7C). These data indicate that sphingolipid enrichment is not required for targeting the DRM-associated protein calflagin to the flagellum, but that sphingolipids are important for DRM maintenance in the bloodstream albeit not in procyclic forms of the parasite.

Discussion

Studies in eukaryotic cells point to roles of sphingolipids as structural membrane components, in regulation of endocytosis and exocytosis, formation of lipid rafts, cell cycle regulation, heat shock response and apoptosis (Bagnat et al., 2001; Bagnat et al., 2000; Hanada, 2003; Obeid et al., 2002). In examining the requirement of sphingolipids in the physiology of procyclic *T. brucei*, we found that *TbSPT2* gene expression and de novo sphingolipid biosynthesis are essential for cell survival and, most notably, impacts cellular proliferation and cytokinesis rather than vesicular trafficking and raft formation. This implicates sphingolipids in cell-cycle-associated signaling in this parasite.

Sphingolipid biosynthesis

Inhibition of TbSPT2 reduces de novo biosynthesis of ceramide and substantially reduces the levels of IPCs in the procyclic cell. In this study, we identified several IPC species: C14:0/d18:1-IPC (*m/z* 750.5), C14:0/d18:0-IPC (*m/z* 752.5), C16:0/d18:1-IPC (*m/z* 778.5) and C16:0/d18:0-IPC (*m/z* 780.5), as well as a minor ion species C18:0/d18:1-IPC (*m/z* 806.6). The first four species are consistent with those reported previously, where the *m/z* values were assigned as C32:1-IPC, C32:0-IPC, C34:1-IPC and C34:0-IPC, respectively (Guther et al., 2006). TbSPT2 RNAi parasites attempt to compensate for the loss of IPCs by increasing the synthesis of several PC species as well as the previously identified 1-O-C18:0-alkyl-2-O-18:2-acyl-PI (Guther et al., 2006) that are not abundant in the parental cells. Further, an increase in the levels of cholesterol and cholesteryl esters upon TbSPT2 RNAi induction and myriocin treatment, presumably by increased cholesterol uptake, suggests another mechanism of compensation for bulk loss of sphingolipids. Cells treated with sterol biosynthesis inhibitors can increase the uptake of exogenous cholesterol from lipid enriched medium (Coppens and Courtoy, 1995; Coppens and Courtoy, 2000; Guther et al., 2006; Neu et al., 1997). Altough we did not detect much ergosterol equal amounts of its precursor lanosterol were detected in all samples, suggesting that ergosterol is synthesized but not detected owing to differences in the extraction and analysis methods employed by us and others (Zhou et al., 2007). Sphingolipid depletion can be complemented with the sphingoid base 3-KDS, indicating that, similarly to *L. major* and yeast, *T. brucei* can scavenge sphingolipids from the medium.

Interestingly, the requirement for SPT2 activity and de novo sphingolipid synthesis in cell survival distinguishes *T. brucei* from the related kinetoplastid protozoan *L. major* (Denny et al., 2004; Denny and Smith, 2004; Zhang et al., 2005; Zhang et al., 2007; Zhang et al., 2003), where sphingoid bases are used primarily for the formation of ethanolamine. Ethanolamine is probably, in part, used for the synthesis of phosphatidylethanolamine via the Kennedy pathway (Zhang et al., 2007), because PE is greatly enriched in

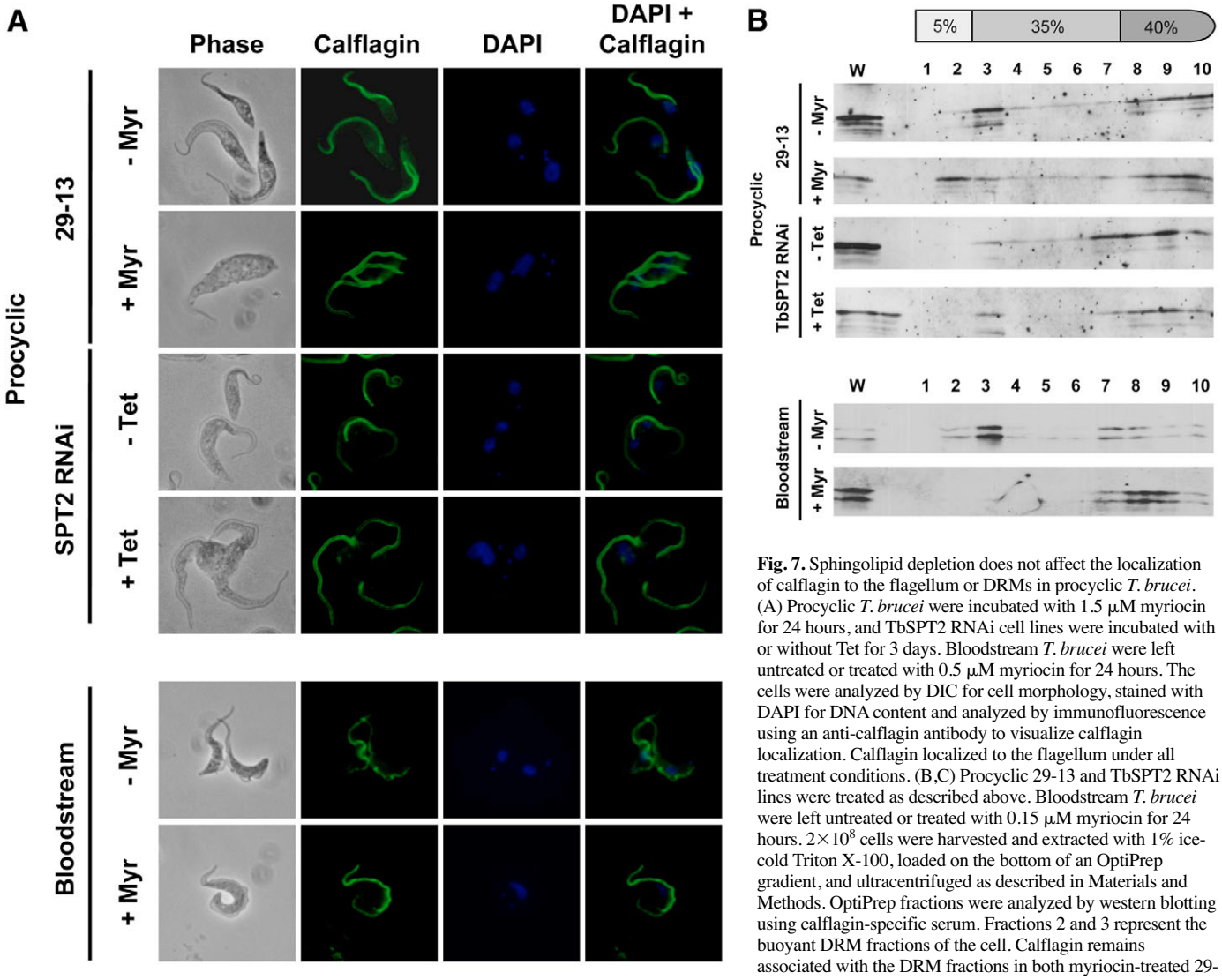

Fig. 7. Sphingolipid depletion does not affect the localization of calflagin to the flagellum or DRMs in procyclic *T. brucei*. (A) Procyclic *T. brucei* were incubated with 1.5 μM myriocin for 24 hours, and TbSPT2 RNAi cell lines were incubated with or without Tet for 3 days. Bloodstream *T. brucei* were left untreated or treated with 0.5 μM myriocin for 24 hours. The cells were analyzed by DIC for cell morphology, stained with DAPI for DNA content and analyzed by immunofluorescence using an anti-calflagin antibody to visualize calflagin localization. Calflagin localized to the flagellum under all treatment conditions. (B,C) Procyclic 29-13 and TbSPT2 RNAi lines were treated as described above. Bloodstream *T. brucei* were left untreated or treated with 0.15 μM myriocin for 24 hours. 2×10^8 cells were harvested and extracted with 1% ice-cold Triton X-100, loaded on the bottom of an OptiPrep gradient, and ultracentrifuged as described in Materials and Methods. OptiPrep fractions were analyzed by western blotting using calflagin-specific serum. Fractions 2 and 3 represent the buoyant DRM fractions of the cell. Calflagin remains associated with the DRM fractions in both myriocin-treated 29-13 and RNAi +Tet cells as well as the controls, but is lost in bloodforms upon treatment with myriocin.

Leishmania membranes during promastigote differentiation. However, addition of exogenous ethanolamine cannot rescue the SPT2 defect in *T. brucei* procyclic cells (data not shown) or bloodstream forms (Sutterwala et al., 2007), and suggests that in this parasite, unlike in *Leishmania*, sphingolipids and long-chain bases themselves rather than their metabolites are indispensable.

Sphingolipids and cell cycle progression in *T. brucei*

Despite inhibition of sphingolipid synthesis, parasites progress through multiple rounds of DNA replication, but are compromised in their ability to correctly complete cytokinesis due to impaired cleavage furrow progression and defects in kinetoplast segregation. A pleomorphic phenotype results from perturbations of several cell cycle events. At early timepoints, we observed dividing cells with a stable cleavage furrow that persisted through DNA replication, a phenotype similar to that reported in *T. brucei* for receptor for activated C kinase 1 (TRACK1) RNAi lines (Rothberg et al., 2006). In others, cytokinesis was completed, but mispositioning of the cleavage furrow resulted in anucleate cells and their complements. Cells with an unseparated enlarged kinetoplast and a detached daughter flagellum became apparent at later timepoints, suggesting that kinetoplast and basal body segregation are also affected by sphingolipid depletion. Presumably, these cells did not initiate cytokinesis, which heavily depends on correct mitochondrial DNA segregation and flagellar attachment (LaCount et al., 2002; Robinson and Gull, 1991), but re-replicated their DNA, as has previously been reported (Hammarton et al., 2007; LaCount et al., 2002). This uncoupling of mitosis and cytokinesis is consistent with reports showing that the cytokinesis checkpoint present in other eukaryotes is not functional in trypanosomes (Ellis et al., 2004; Grellier et al., 1999; Ngo et al., 1998; Rothberg et al., 2006). The number of parasites with multiple DNA and flagellar content increased after prolonged TbSPT2 RNAi induction or treatment with high concentrations of myriocin. Enlarged kinetoplasts and detached flagella were observed in some of the cells as well, suggesting that this defect was secondary to, or concurrent with, completion of cleavage furrow ingression. Further, the distention of mitochondrial membrane and multilamellar structures within the kinetoplast membrane may have contributed to problems with kinetoplast segregation.

Overall, this phenotype is consistent with the notion that sphingoid bases function as second messengers in stimulation of both mitogenesis and cell proliferation. In mammalian cells, long-chain bases downstream of 3-KDS have been shown to promote or inhibit cell cycle progression via ERK and JNK kinases (Coroneos et al., 1996; Pyne et al., 1996). The sphingolipid psychosine (galactosylsphingosine) triggers the inhibition and reversal of partially completed cytokinesis, and the induction of multinuclear giant cells associated with a sphingolipid metabolic disease, globoid cell leukodystrophy (Kanazawa et al., 2000). Inhibition of sphingolipid biosynthesis by myriocin also induces multinucleation, possibly by signaling via a downstream serine/threonine kinase SLI2, which is regulated by intracellular sphingolipid levels (Kozutsumi et al., 2002). Further, sphingolipid-enriched signaling platforms promote activation of kinases Src and PLCγ which are essential to cytokinesis (Ng et al., 2005). However, myriocin treatment of bloodform *T. brucei* does not inhibit cytokinesis but rather arrests cell growth and replication in all stages of the cell cycle (Sutterwala et al., 2007).

Although we did not observe differences in the association of calflagin with lipid rafts in procyclic *T. brucei*, we cannot discount that changes in membrane sphingolipid and raft composition may affect other proteins with differing affinities for membrane lipid environments. One report indicates that the Polo-like kinase TbPLK localizes to the cleavage furrow in *T. brucei* (Kumar and Wang, 2006), although a subsequent study suggests that its localization is cytoplasmic (Hammarton et al., 2007). Our phenotype suggests that perturbation of this and other kinases is responsible in part for the defects in kinetoplast and basal body migration (Kumar and Wang, 2006). It is also interesting to note that removal of an autoregulatory domain of the ERK-like, CRK-like protein kinase TbECK1 results in large cells with a DNA content of >4C.

Intriguingly, *T. brucei* is more similar to yeast than to *L. major* in its requirement of sphingoid bases for cell cycle progression. In *S. cerevisiae* SPT mutants, dry-mass accumulation and protein synthesis continue after sphingolipid biosynthesis stops (Pinto et al., 1992), whereas *L. major* log-phase promastigotes do not require sphingolipids to complete the cell cycle. Because no gross endocytosis or exocytosis defects are evident early after SPT2 inhibition in *T. brucei*, one or more sphingoid intermediates are likely to play a signaling role in *T. brucei*.

Vesicular trafficking defects and DRMs

Sphingolipid biosynthesis is required for efficient transport of GPI-anchored membrane proteins in *S. cerevisiae* (Bagnat et al., 2001; Obeid et al., 2002) but does not affect the transport of GPI-anchored VSG in bloodstream *T. brucei* or HeLa cells, indicating that this requirement for exocytosis is not universal (Sutterwala et al., 2007). Further, the canonical requirement for sphingolipids in the formation of DRM in eukaryotic cells (Brown and London, 1998; Ikonen, 2001; Simons and Toomre, 2000; van Meer and Lisman, 2002) has been challenged in *Leishmania*, where the association of GPI-anchored protein gp63 with DRMs is not affected in SPT2-null promastigotes (Denny et al., 2001; Denny et al., 2004; Zhang et al., 2003). We confirmed that sphingolipids are not essential for exocytosis and DRM maintenance, by showing that in procyclic cells, flagellar localization and DRM targeting of the dually acylated membrane protein calflagin is not affected by TbSPT2 RNAi induction or myriocin treatment. However, altough calflagin is still targeted to the flagellum in myriocin-treated bloodstream forms, its association with DRMs is compromised.

The differences in membrane composition between the two *T. brucei* stages provide a likely explanation for this phenomenon. Ergosterol, found in membranes of most kinetoplastids including procyclic but not bloodstream *T. brucei* (Coppens and Courtoy, 1995; Coppens and Courtoy, 2000), forms larger and more thermostable rafts than cholesterol (Xu et al., 2001). The abundance of ergosterol and raft-associated GPI-anchored moieties in the *Leishmania* membrane may allow the parasites to retain lipid rafts even in the absence of sphingolipids (Denny et al., 2004; Zhang et al., 2005; Zhang et al., 2003). Whereas the surface coat of *T. brucei* in both life cycle stages also contains an abundance of GPI-linked proteins, these do not associate with DRMs when extracted with ice-cold 1% Triton X-100 (Denny et al., 2001) (our unpublished work). However, ergosterol and additional cholesterol scavenged by the TbSPT2 RNAi line and by myriocin-treated cells might provide an environment that can support the DRM association of calflagin in the procyclic membrane. Similarly, the *Leishmania* flagellar membrane protein SMP-1 remains associated with DRMs after myriocin treatment, but not after a combined myriocin and sterol inhibitor treatment (Tull et al., 2004). However, lack of ergosterol and a greater sensitivity to sphingolipid depletion might not allow the bloodstream forms to properly maintain DRM integrity. Concordantly, depletion of cholesterol via methyl-β-cyclodextrin from bloodstream forms also causes loss of DRM association (our unpublished work).

Whereas some vesicular trafficking defects emerged after prolonged TbSPT2 RNAi induction, they are not severe and may be secondary to cell disruption because of excessive growth without division. We observed an increased number of lipid bodies in TbSPT2 cells, previously seen in *Leishmania* SPT2-null promastigotes (Denny et al., 2004; Zhang et al., 2003) and in aureobasidin-A-treated *T. cruzi* (Salto et al., 2003); however, the increased uptake of cholesterol may account for some of this defect. We also observed some disrupted Golgi complexes in cells that showed other abnormalities. We did not, however, notice any increased vacuolization, cytoplasmic or flagellar pocket-vesicle accumulation, or empty acidocalcisomes indicative of severe vesicular trafficking defects in differentiating SPT2-null *Leishmania* (Denny et al., 2004; Denny and Smith, 2004; Zhang et al., 2005; Zhang et al., 2003). Perhaps the demands on the vesicular trafficking pathway in growing procyclic cells remain constant, like in log-phase promastigotes of *L. major*. It is possible that molecules necessary for the fusion of secretory vesicles with the plasma membrane are affected by sphingolipid depletion, as has been proposed for v-SNAREs and t-SNAREs in yeast (Dickson and Lester, 1999). If so, this may also account for the failure of some flagellar pockets and mitochondria to divide.

Synthesis of sphingolipid bases is also required for endocytosis in the bloodstream form of *T. brucei*, although the effect of its depletion is mild (Sutterwala et al., 2007). *T. brucei* cells in which levels of actin or clathrin heavy chain are knocked down using RNAi develop greatly enlarged flagellar pockets (bloodstream forms) or distention of Golgi cisternae (procyclic forms) (Allen et al., 2003; Garcia-Salcedo et al., 2004), and accumulation of vesicles in various locations within the cytoplasm. The Golgi remained largely unaffected in many procyclic parasites, and no accumulation of vesicles in the cytoplasm was seen in any cell with a structurally intact membrane and organelles. An assay to determine the uptake of transferrin did not detect any difference in

myriocin or TbSPT2-RNAi-induced cell lines (data not shown). This suggests that endocytic defects resulting from sphingolipid depletion in the procyclic stage of the parasite are mild as well. The observed multilamellar structure by the nucleus might be an enlarged lysosome originating from membrane mistargeting (Sutterwala et al., 2007). Likewise, similar structures have been reported in cells that undergo autophagy after inhibition of sterol synthesis (Coppens and Courtoy, 1995). Enlarged flagellar pockets and mitochondrial pocket distention have been reported in dying trypanosome cells (Figarella et al., 2005; Lazardi et al., 1990; Pearson et al., 2000; Welburn et al., 1996), although mitochondrial distention might also be due to sensitivity of the trypanosome mitochondrial membrane to lipid perturbation, as has been observed after ergosterol depletion (Coppens and Courtoy, 2000).

Future studies focusing on the enzymes downstream of SPT in the sphingolipid pathway will help determine which long-chain-base intermediate is responsible for the specific defects observed in the TbSPT2 RNAi line, and should help to determine which other observed defects are be cell-cycle independent. Identification and characterization of the cell-cycle-mediating effector kinases that may be regulated by sphingolipids is also worthy of careful analysis.

Materials and Methods

Parasite culture

T. brucei procyclic strain 29-13 (Wirtz and Clayton, 1995) was maintained at 27°C in SDM79 medium supplemented with 10% FCS, 25 μg/ml hygromycin and 25 μg/ml G418, as previously described (Wang et al., 2000). This strain of *T. brucei* contains the genes expressing T7 RNA polymerase and the Tet-repressor protein, allowing induction with tetracycline from two T7 promoters. Procyclic transfectants were maintained in SDM79 supplemented with 50 μg/ml hygromycin, 15 μg/ml G418 and 2.5 μg/ml phleomycin as needed. The *T. brucei* single-marker bloodstream form strain 90-13 (Biebinger et al., 1997) was grown in HMI-9 medium at 37°C.

Reagents and antibodies

4′,6-diamidino-2-phenylindole (DAPI), Hoechst DNA dyes and myriocin were obtained from Sigma. 3-ketodihydrosphingosine (3-KDS), C-18 ceramide and mixed ceramides were obtained from Matreya (Pleasant Gap, PA). PFR-specific mouse antiserum ROD-1 (Woods et al., 1989) was the kind gift of K. Gull. Calflagin Tb1.7 polyclonal mouse serum was generated as described (Olson et al., 1994). Secondary antibodies Alexa-Fluor-488-conjugated goat anti-mouse IgG (Invitrogen, Carlsbad, CA) and horseradish-peroxidase-conjugated goat anti-mouse IgG (KPL) were used for immunofluorescence microscopy and western blotting, respectively.

DNA constructs

The *T. brucei* SPT2 gene was identified through a search of the Sanger *T. brucei* database (www.genedb.org). The 1674 bp gene was identified with a temporary systematic ID of Tb10.70.3220 as of February 26, 2005. The *T. brucei* SPT2 735 bp RNAi fragment was verified for specificity by the *RNA-it* program (Redmond et al., 2003), generated from 29-13 strain genomic DNA by polymerase chain reaction amplification using primers 5′-AAGGCAGTAACTGAAGCCGA-3′ and 5′-CAAGCTATCGCTGACCACAA-3′, and ligated into the pCRII-TOPO vector (Invitrogen, Carlsbad, CA). The RNAi fragment was directionally subcloned using *Xho*I and *Hin*dIII into the RNAi vector pZJM (Wang et al., 2000), which supports expression of double-stranded (ds) RNA from Tet-inducible T7 promoters.

RNA interference in *T. brucei* procyclic forms

To transform trypanosomes, mid-log-phase 29-13 strain parasites were electroporated with 50 μg of pZJM-TbSPT2 DNA linearized with *Cla*I, using a Gene Pulser (Bio-Rad, Hercules, CA) as previously described (Wang et al., 2000). Transfectants were selected with 2.5 μg/ml phleomycin and single-cell clones were isolated by limiting dilution cloning. The expression of dsRNA was induced by addition of 1 μg/ml Tet to parasites diluted to 10^6 cells/ml in SDM79 medium. Four clones (TbSPT2-1, TbSPT2-2, TbSPT2-3 andTbSPT2-4) were shown to have similar growth kinetics and morphology upon Tet induction, and TbSPT2-2 was used in all experiments.

Growth studies

Logarithmically growing procyclic cultures were seeded at a density of 10^6 cells/ml, and diluted to the same concentration daily. TbSPT2 RNAi lines were induced to express RNAi after addition of Tet to 1 μg/ml. Cell density was determined using a Coulter counter (Beckman Coulter, Fullerton, CA) at the indicated times. The growth studies were repeated three times. Where indicated, cells were complemented daily with sphingoid bases 3-KDS, C-18 ceramide and mixed ceramides.

Immunofluorescence microscopy

Cells were washed twice in PBS and settled onto poly-L-lysine coated slides for 30 minutes on ice, fixed with 4% paraformaldehyde for 30 minutes, permeabilized with 0.2% Triton X-100 and blocked with PBS with 1% bovine serum albumin and 2% normal goat serum. Cells were incubated with wither paraflagellar rod-specific (Rod1) mouse serum (1:4 dilution) or calflagin-specific mouse serum (1:1000 dilution) overnight and with Alexa-Fluor-488-conjugated goat anti-mouse IgG (1:200 dilution) for 2 hours; a wash of 5 minutes with PBS followed each antibody incubation. 2 μg/ml DAPI dissolved in water was applied to cells for 1 minute before mounting with Gelvatol mounting medium. Cells were visualized with Leica Inverted Microscope using Openlab software (Leica Microcystems, Bannockburn, IL).

Cell cycle analysis

To assess DNA content, TbSPT2 RNAi cells were collected at different times following RNAi induction, washed twice with PBS and resuspended in PBS containing 0.1% Triton X-100, 0.5% formaldehyde, and 2 μg/ml Hoechst dye. After an overnight incubation at 4°C, cells were analyzed using an LSRII cell sorter (BD Biosciences, San Jose, CA). Gating was determined for control cells in each experiment, and the same values were used for all treated cells. Cell cycle parameters were analyzed using FACSDiva software (BD Biosciences, San Jose, CA).

Electron microscopy

For TEM, cells were embedded in 2% agar, fixed with 2.5% glutaraldehyde in 100 mM sodium cacodylate buffer, and post-fixed with 1% osmium tetroxide-1.5% potassium ferrocyanide in 100 mM sodium cacodylate buffer for 30 minutes at room temperature. After three changes of buffer, the pellet was stained with 2.5% uranyl acetate and dehydrated in ethanol, then embedded in Epon 812 resin and sectioned on a Reichert Ultracut ultramicrotome using a diamond knife. Sections were collected onto grids and stained with uranyl acetate and lead citrate for contrast. Grids were examined using the JEOL 100CX transmission electron microscope. For SEM, cells were immobilized on poly-L-lysine-coated silicon wafers, fixed and dehydrated as described above, and critical-point dried. The wafers were placed into specimen mounts using carbon tape, coated with gold in a Bal-Tec Med 020 with single ‘cool’ sputter device, and examined in a Hitachi S4500-II cold-field emission-scanning microscope, as previously described (McGwire et al., 2003).

Thin-layer chromatography

Thin-layer chromatography (TLC) was performed essentially as described (Zhang et al., 2003). Briefly, 3×10^8 *T. brucei* cells were radiolabeled by addition of [^{3}H]serine (29.5 Ci/mmol) at 20 μCi/ml to the culture for 40 minutes at room temperature. Cells were harvested, washed twice with PBS, and extracted with 3.75 volumes of $CHCl_3$/methanol (1:2), followed by 1.25 volumes of $CHCl_3$ and 1.25 volumes of water. After centrifugation at 1000 ***g*** for 10 minutes, the upper aqueous phase was removed and discarded. The organic phase was washed once with water, dried under nitrogen and dissolved in $CHCl_3$ at the equivalent of 10^9 cells/ml. Lipid concentration was normalized to protein content using Bio-Rad Protein Assay. TLC analysis of lipids was performed using Silica Gel 60 A TLC plates (Whatman, Middlesex, UK), using solvent containing methylacetate:1-propanol:CHCl3:methanol:KCl (0.25%) at 25:25:25:10:9. Autoradiography was performed after spraying plates with En^{3}Hance (Perkin Elmer, Waltham, MA).

Mass spectrometry of lipid extracts

Cells of the 29-13 cell line were either left untreated or treated with 1.5 μM myriocin for 24 hours, and the TbSPT2 RNAi lines were grown with and without Tet (1 μg/ml) for 3 days. 1×10^9 cells of each type were extracted using a modified Folch’s method (Folch et al., 1957). Specifically, cells were washed and resuspended in 0.2 ml PBS and extracted a total of three times with 2 ml of chloroform:methanol (2:1) by vortexing and centrifugation at 1000 ***g*** for 5 minutes; 1 ml H_2O was added to 6 ml of the chloroform:methanol (2:1) following the extraction. The solution was homogenized by vortexing for 1 minute and then centrifuged at 1000 ***g*** for 5 minutes to separate upper and lower phases. The products were dried under a stream of nitrogen, resuspended in chloroform:methanol (1:1) and diluted in chloroform:methanol (1:1) containing 0.1% formic acid and 0.1% NH_4OH for electrospray-ionization mass spectrometry (ESI-MS) The samples were analyzed in negative-ion mode using a Micromass Qtof-1 mass spectrometer (Waters, Milford, MA). Individual ion species were subjected to ESI tandem-mass-spectrometry (ESI-MS/MS) using collision energy of 27-50 eV. MS/MS spectra were analyzed manually to identify sphingolipid and phospholipid molecular species.

Quantification of sterol fractions by GC-MS

For sterol analysis by GC-MS, cells of 29-13, 29-13+Myr, SPT2 (–Tet), and SPT2 (+Tet) cell lines were each grown to a density of 1×10^8 and total lipids extracted as described above. Extracts were dried under nitrogen, resuspended in 1 ml

chloroform (100%) and loaded onto silica columns manufactured in a Pasteur pipette, using very fine glass wool and ~100 mg of silica gel resin (pore size 60 Å, 200-400 μm mesh, Sigma). Columns were pre-equilibrated with chloroform (100%) and, following loading, the sterol fraction was eluted with 4 ml chloroform (100%). The fractions were spiked with β-sitosterol (Sit) (100 ng) (Sigma-Aldrich), used as internal standard, and dried under nitrogen stream. Each sample was resuspended in 10 μl of dichloromethane and 1 μl was used for the analysis by gas chromatography (Trace GC, Thermo Fisher, Austin, TX) coupled to mass spectrometry (Polaris Q, Thermo Fisher) (GC-MS). The separation was performed in a TR-5ms column (30 m × 250 μm × 0.25 μm, Thermo Fisher). The injector was set at 250°C and the gradient was as follows: 3 minutes at 170°C, 20°C/minute increase to 280°C, followed by 17-minute hold. Helium was used as a carrier with a flow rate of 1.2 ml/min. The molecules were ionized by electron impact at 70 eV and 200°C. The spectra were collected at the 50-650 *m/z* range. Chromatograms were generated by plotting the spectra of diagnostic fragment-ion species at *m/z* 368, 386, 396, 412 and 426, for cholesteryl ester (ChoE), cholesterol (Cho), ergosterol (Erg), Sit and lanosterol (Lan), respectively. Quantification was done using an external standard curve (1-100 ng; normalized with 10 ng Sit as internal standard) for Cho, Erg and Lan.

Preparation of detergent-resistant membranes

DRMs were purified by flotation of the cell protein extracts of 2×10^8 cells through a 5%-35%-40% Optiprep™ density gradient followed by ultracentrifugation essentially as described (Bagnat et al., 2000) (our unpublished work). Fractions were collected and analyzed by SDS-PAGE and immunoblotted with calflagin-specific polyclonal mouse serum (1:1000) using standard methods.

We are grateful to Jayme Borensztajn and Tao Fu for reagents and technical advice, Kathryn Buchanan and Brian Emmer for helpful discussions and critical reading of the manuscript, and the staff of the Biomolecule Analysis Core Facility at the University of Texas at El Paso. This work was supported in part through grant AI46781 from the U.S. Public Health Service and by NCRR grant 5G12RR008124 to the Border Biomedical Research Center at the University of Texas at El Paso. A.F. was supported in part by a predoctoral fellowship from the American Heart Association.

References

Alibu, V. P., Storm, L., Haile, S., Clayton, C. and Horn, D. (2005). A doubly inducible system for RNA interference and rapid RNAi plasmid construction in *Trypanosoma brucei*. *Mol. Biochem. Parasitol.* **139**, 75-82.

Allen, C. L., Goulding, D. and Field, M. C. (2003). Clathrin-mediated endocytosis is essential in *Trypanosoma brucei*. *EMBO J.* **22**, 4991-5002.

Bagnat, M. and Simons, K. (2002). Lipid rafts in protein sorting and cell polarity in budding yeast *Saccharomyces cerevisiae*. *Biol. Chem.* **383**, 1475-1480.

Bagnat, M., Keranen, S., Shevchenko, A. and Simons, K. (2000). Lipid rafts function in biosynthetic delivery of proteins to the cell surface in yeast. *Proc. Natl. Acad. Sci. USA* **97**, 3254-3259.

Bagnat, M., Chang, A. and Simons, K. (2001). Plasma membrane proton ATPase Pma1p requires raft association for surface delivery in yeast. *Mol. Biol. Cell* **12**, 4129-4138.

Benting, J., Rietveld, A., Ansorge, I. and Simons, K. (1999). Acyl and alkyl chain length of GPI-anchors is critical for raft association *in vitro*. *FEBS Lett.* **462**, 47-50.

Bertello, L. E., Goncalvez, M. F., Colli, W. and de Lederkremer, R. M. (1995). Structural analysis of inositol phospholipids from *Trypanosoma cruzi* epimastigote forms. *Biochem. J.* **310**, 255-261.

Biebinger, S., Wirtz, L. E., Lorenz, P. and Clayton, C. (1997). Vectors for inducible expression of toxic gene products in bloodstream and procyclic *Trypanosoma brucei*. *Mol. Biochem. Parasitol.* **85**, 99-112.

Briggs, L. J., McKean, P. G., Baines, A., Moreira-Leite, F., Davidge, J., Vaughan, S. and Gull, K. (2004). The flagella connector of *Trypanosoma brucei*: an unusual mobile transmembrane junction. *J. Cell Sci.* **117**, 1641-1651.

Brown, D. A. and London, E. (1998). Functions of lipid rafts in biological membranes. *Annu. Rev. Cell Dev. Biol.* **14**, 111-136.

Coppens, I. and Courtoy, P. J. (1995). Exogenous and endogenous sources of sterols in the culture-adapted procyclic trypomastigotes of *Trypanosoma brucei*. *Mol. Biochem. Parasitol.* **73**, 179-188.

Coppens, I. and Courtoy, P. J. (2000). The adaptative mechanisms of *Trypanosoma brucei* for sterol homeostasis in its different life-cycle environments. *Annu. Rev. Microbiol.* **54**, 129-156.

Coroneos, E., Wang, Y., Panuska, J. R., Templeton, D. J. and Kester, M. (1996). Sphingolipid metabolites differentially regulate extracellular signal-regulated kinase and stress-activated protein kinase cascades. *Biochem. J.* **316**, 13-17.

Denny, P. W. and Smith, D. F. (2004). Rafts and sphingolipid biosynthesis in the kinetoplastid parasitic protozoa. *Mol. Microbiol.* **53**, 725-733.

Denny, P. W., Field, M. C. and Smith, D. F. (2001). GPI-anchored proteins and glycoconjugates segregate into lipid rafts in Kinetoplastida. *FEBS Lett.* **491**, 148-153.

Denny, P. W., Goulding, D., Ferguson, M. A. and Smith, D. F. (2004). Sphingolipid-free *Leishmania* are defective in membrane trafficking, differentiation and infectivity. *Mol. Microbiol.* **52**, 313-327.

Dickson, R. C. and Lester, R. L. (1999). Yeast sphingolipids. *Biochim. Biophys. Acta* **1426**, 347-357.

Ellis, J., Sarkar, M., Hendriks, E. and Matthews, K. (2004). A novel ERK-like, CRK-like protein kinase that modulates growth in *Trypanosoma brucei* via an autoregulatory C-terminal extension. *Mol. Microbiol.* **53**, 1487-1499.

Figarella, K., Rawer, M., Uzcategui, N. L., Kubata, B. K., Lauber, K., Madeo, F., Wesselborg, S. and Duszenko, M. (2005). Prostaglandin D2 induces programmed cell death in *Trypanosoma brucei* bloodstream form. *Cell Death Differ.* **12**, 335-346.

Folch, J., Lees, M. and Sloane Stanley, G. H. (1957). A simple method for the isolation and purification of total lipides from animal tissues. *J. Biol. Chem.* **226**, 497-509.

Funato, K., Vallee, B. and Riezman, H. (2002). Biosynthesis and trafficking of sphingolipids in the yeast *Saccharomyces cerevisiae*. *Biochemistry* **41**, 15105-15114.

Garcia-Salcedo, J. A., Perez-Morga, D., Gijon, P., Dilbeck, V., Pays, E. and Nolan, D. P. (2004). A differential role for actin during the life cycle of *Trypanosoma brucei*. *EMBO J.* **23**, 780-789.

Grellier, P., Sinou, V., Garreau-de Loubresse, N., Bylen, E., Boulard, Y. and Schrevel, J. (1999). Selective and reversible effects of vinca alkaloids on *Trypanosoma cruzi* epimastigote forms: blockage of cytokinesis without inhibition of the organelle duplication. *Cell Motil. Cytoskeleton* **42**, 36-47.

Gruenberg, J. (2001). The endocytic pathway: a mosaic of domains. *Nat. Rev. Mol. Cell Biol.* **2**, 721-730.

Guther, M. L., Lee, S., Tetley, L., Acosta-Serrano, A. and Ferguson, M. A. (2006). GPI-anchored proteins and free GPI glycolipids of procyclic form *Trypanosoma brucei* are nonessential for growth, are required for colonization of the tsetse fly, and are not the only components of the surface coat. *Mol. Biol. Cell* **17**, 5265-5274.

Hammarton, T. C., Kramer, S., Tetley, L., Boshart, M. and Mottram, J. C. (2007). *Trypanosoma brucei* Polo-like kinase is essential for basal body duplication, kDNA segregation and cytokinesis. *Mol. Microbiol.* **65**, 1229-1248.

Hanada, K. (2003). Serine palmitoyltransferase, a key enzyme of sphingolipid metabolism. *Biochim. Biophys. Acta* **1632**, 16-30.

Hanada, K., Nishijima, M., Kiso, M., Hasegawa, A., Fujita, S., Ogawa, T. and Akamatsu, Y. (1992). Sphingolipids are essential for the growth of Chinese hamster ovary cells. Restoration of the growth of a mutant defective in sphingoid base biosynthesis by exogenous sphingolipids. *J. Biol. Chem.* **267**, 23527-23533.

Ikonen, E. (2001). Roles of lipid rafts in membrane transport. *Curr. Opin. Cell Biol.* **13**, 470-477.

Jenkins, G. M. and Hannun, Y. A. (2001). Role for *de novo* sphingoid base biosynthesis in the heat-induced transient cell cycle arrest of *Saccharomyces cerevisiae*. *J. Biol. Chem.* **276**, 8574-8581.

Kanazawa, T., Nakamura, S., Momoi, M., Yamaji, T., Takematsu, H., Yano, H., Sabe, H., Yamamoto, A., Kawasaki, T. and Kozutsumi, Y. (2000). Inhibition of cytokinesis by a lipid metabolite, psychosine. *J. Cell Biol.* **149**, 943-950.

Kohl, L., Robinson, D. and Bastin, P. (2003). Novel roles for the flagellum in cell morphogenesis and cytokinesis of trypanosomes. *EMBO J.* **22**, 5336-5346.

Kozutsumi, Y., Kanazawa, T., Sun, Y., Yamaji, T., Yamamoto, H. and Takematsu, H. (2002). Sphingolipids involved in the induction of multinuclear cell formation. *Biochim. Biophys. Acta* **1582**, 138-143.

Kumar, P. and Wang, C. C. (2006). Dissociation of cytokinesis initiation from mitotic control in a eukaryote. *Eukaryotic Cell* **5**, 92-102.

LaCount, D. J., Barrett, B. and Donelson, J. E. (2002). *Trypanosoma brucei* FLA1 is required for flagellum attachment and cytokinesis. *J. Biol. Chem.* **277**, 17580-17588.

Lazardi, K., Urbina, J. A. and de Souza, W. (1990). Ultrastructural alterations induced by two ergosterol biosynthesis inhibitors, ketoconazole and terbinafine, on epimastigotes and amastigotes of *Trypanosoma (Schizotrypanum) cruzi*. *Antimicrob. Agents Chemother.* **34**, 2097-2105.

McGwire, B. S., Olson, C. L., Tack, B. F. and Engman, D. M. (2003). Killing of African trypanosomes by antimicrobial peptides. *J. Infect. Dis.* **188**, 146-152.

Miyake, Y., Kozutsumi, Y., Nakamura, S., Fujita, T. and Kawasaki, T. (1995). Serine palmitoyltransferase is the primary target of a sphingosine-like immunosuppressant, ISP-1/myriocin. *Biochem. Biophys. Res. Commun.* **211**, 396-403.

Moreira-Leite, F. F., Sherwin, T., Kohl, L. and Gull, K. (2001). A trypanosome structure involved in transmitting cytoplasmic information during cell division. *Science* **294**, 610-612.

Neu, E., Hemmerich, P. H., Peter, H. H., Krawinkel, U. and von Mikecz, A. H. (1997). Characteristic epitope recognition pattern of autoantibodies against eukaryotic ribosomal protein L7 in systemic autoimmune diseases. *Arthritis Rheum.* **40**, 661-671.

Ng, M. M., Chang, F. and Burgess, D. R. (2005). Movement of membrane domains and requirement of membrane signaling molecules for cytokinesis. *Dev. Cell* **9**, 781-790.

Ngo, H., Tschudi, C., Gull, K. and Ullu, E. (1998). Double-stranded RNA induces mRNA degradation in *Trypanosoma brucei*. *Proc. Natl. Acad. Sci. USA* **95**, 14687-14692.

Obeid, L. M., Okamoto, Y. and Mao, C. (2002). Yeast sphingolipids: metabolism and biology. *Biochim. Biophys. Acta* **1585**, 163-171.

Olson, C. L., Nadeau, K. C., Sullivan, M. A., Winquist, A. G., Donelson, J. E., Walsh, C. T. and Engman, D. M. (1994). Molecular and biochemical comparison of the 70 kDa heat shock proteins of *Trypanosoma cruzi*. *J. Biol. Chem.* **269**, 3868-3874.

Patnaik, P. K., Field, M. C., Menon, A. K., Cross, G. A., Yee, M. C. and Butikofer, P. (1993). Molecular species analysis of phospholipids from *Trypanosoma brucei* bloodstream and procyclic forms. *Mol. Biochem. Parasitol.* **58**, 97-105.

Pearson, T. W., Beecroft, R. P., Welburn, S. C., Ruepp, S., Roditi, I., Hwa, K. Y., Englund, P. T., Wells, C. W. and Murphy, N. B. (2000). The major cell surface glycoprotein procyclin is a receptor for induction of a novel form of cell death in African trypanosomes *in vitro*. *Mol. Biochem. Parasitol.* **111**, 333-349.

Pepin, J. (2007). Combination therapy for sleeping sickness: a wake-up call. *J. Infect. Dis.* **195**, 311-313.

Perry, D. K. (2002). Serine palmitoyltransferase: role in apoptotic *de novo* ceramide synthesis and other stress responses. *Biochim. Biophys. Acta* **1585**, 146-152.
Pike, L. J. (2003). Lipid rafts: bringing order to chaos. *J. Lipid Res.* **44**, 655-667.
Pinto, W. J., Srinivasan, B., Shepherd, S., Schmidt, A., Dickson, R. C. and Lester, R. L. (1992). Sphingolipid long-chain-base auxotrophs of *Saccharomyces cerevisiae*: genetics, physiology, and a method for their selection. *J. Bacteriol.* **174**, 2565-2574.
Ploubidou, A., Robinson, D. R., Docherty, R. C., Ogbadoyi, E. O. and Gull, K. (1999). Evidence for novel cell cycle checkpoints in trypanosomes: kinetoplast segregation and cytokinesis in the absense of mitosis. *J. Cell Sci.* **112**, 4641-4650.
Pyne, S., Chapman, J., Steele, L. and Pyne, N. J. (1996). Sphingomyelin-derived lipids differentially regulate the extracellular signal-regulated kinase 2 (ERK-2) and c-Jun N-terminal kinase (JNK) signal cascades in airway smooth muscle. *Eur. J. Biochem.* **237**, 819-826.
Redmond, S., Vadivelu, J. and Field, M. C. (2003). RNAit: an automated web-based tool for the selection of RNAi targets in *Trypanosoma brucei*. *Mol. Biochem. Parasitol.* **128**, 115-118.
Robinson, D. R. and Gull, K. (1991). Basal body movements as a mechanism for mitochondrial genome segregation in the trypanosome cell cycle. *Nature* **352**, 731-733.
Robinson, D. R., Sherwin, T., Ploubidou, A., Byard, E. H. and Gull, K. (1995). Microtubule polarity and dynamics in the control of organelle positioning, segregation, and cytokinesis in the trypanosome cell cycle. *J. Cell Biol.* **128**, 1163-1172.
Rothberg, K. G., Burdette, D. L., Pfannstiel, J., Jetton, N., Singh, R. and Ruben, L. (2006). The RACK1 homologue from *Trypanosoma brucei* is required for the onset and progression of cytokinesis. *J. Biol. Chem.* **281**, 9781-9790.
Simons, K. and Toomre, D. (2000). Lipid rafts and signal transduction. *Nat. Rev. Mol. Cell Biol.* **1**, 31-39.
Sutterwala, S. S., Creswell, C. H., Sanyal, S., Menon, A. K. and Bangs, J. D. (2007). *De novo* sphingolipid synthesis is essential for viability, but not transport of GPI-anchored proteins, in African trypanosomes. *Eukaryot. Cell* **6**, 454-464.
Treumann, A., Zitzmann, N., Hulsmeier, A., Prescott, A. R., Almond, A., Sheehan, J. and Ferguson, M. A. (1997). Structural characterisation of two forms of procyclic acidic repetitive protein expressed by procyclic forms of *Trypanosoma brucei*. *J. Mol. Biol.* **269**, 529-547.
Tull, D., Vince, J. E., Callaghan, J. M., Naderer, T., Spurck, T., McFadden, G. I., Currie, G., Ferguson, K., Bacic, A. and McConville, M. J. (2004). SMP-1, a member of a new family of small myristoylated proteins in kinetoplastid parasites, is targeted to the flagellum membrane in *Leishmania*. *Mol. Biol. Cell* **15**, 4775-4786.
Van der Linden, P. W. and Deelder, A. M. (1984). *Schistosoma mansoni*: a diamidinophenylindole probe for *in vitro* death of schistosomula. *Exp. Parasitol.* **57**, 125-131.
van Meer, G. and Lisman, Q. (2002). Sphingolipid transport: rafts and translocators. *J. Biol. Chem.* **277**, 25855-25858.
Vickerman, K. (1985). Developmental cycles and biology of pathogenic trypanosomes. *Br. Med. Bull.* **41**, 105-114.
Wang, Z., Morris, J. C., Drew, M. E. and Englund, P. T. (2000). Inhibition of *Trypanosoma brucei* gene expression by RNA interference using an integratable vector with opposing T7 promoters. *J. Biol. Chem.* **275**, 40174-40179.
Welburn, S. C., Dale, C., Ellis, D., Beecroft, R. and Pearson, T. W. (1996). Apoptosis in procyclic *Trypanosoma brucei rhodesiense in vitro*. *Cell Death Differ.* **3**, 229-236.
Wirtz, E. and Clayton, C. (1995). Inducible gene expression in trypanosomes mediated by a prokaryotic repressor. *Science* **268**, 1179-1183.
Woods, A., Sherwin, T., Sasse, R., MacRae, T. H., Baines, A. J. and Gull, K. (1989). Definition of individual components within the cytoskeleton of *Trypanosoma brucei* by a library of monoclonal antibodies. *J. Cell Sci.* **93**, 491-500.
Xu, X., Bittman, R., Duportail, G., Heissler, D., Vilcheze, C. and London, E. (2001). Effect of the structure of natural sterols and sphingolipids on the formation of ordered sphingolipid/sterol domains (rafts). Comparison of cholesterol to plant, fungal, and disease-associated sterols and comparison of sphingomyelin, cerebrosides, and ceramide. *J. Biol. Chem.* **276**, 33540-33546.
Zanolari, B., Friant, S., Funato, K., Sutterlin, C., Stevenson, B. J. and Riezman, H. (2000). Sphingoid base synthesis requirement for endocytosis in *Saccharomyces cerevisiae*. *EMBO J.* **19**, 2824-2833.
Zhang, K., Showalter, M., Revollo, J., Hsu, F. F., Turk, J. and Beverley, S. M. (2003). Sphingolipids are essential for differentiation but not growth in *Leishmania*. *EMBO J.* **22**, 6016-6026.
Zhang, K., Hsu, F. F., Scott, D. A., Docampo, R., Turk, J. and Beverley, S. M. (2005). *Leishmania* salvage and remodelling of host sphingolipids in amastigote survival and acidocalcisome biogenesis. *Mol. Microbiol.* **55**, 1566-1578.
Zhang, K., Pompey, J. M., Hsu, F. F., Key, P., Bandhuvula, P., Saba, J. D., Turk, J. and Beverley, S. M. (2007). Redirection of sphingolipid metabolism toward de novo synthesis of ethanolamine in Leishmania. *EMBO J.* **26**, 1094-1104.
Zhou, W., Cross, G. A. and Nes, W. D. (2007). Cholesterol import fails to prevent catalyst-based inhibition of ergosterol synthesis and cell proliferation of *Trypanosoma brucei*. *J. Lipid Res.* **48**, 665-673.